
CLIPLoss and Norm-Based Data Selection Methods for Multimodal Contrastive Learning

Yiping Wang*
University of Washington

Yifang Chen*
University of Washington

Wendan Yan
University of Washington

Alex Fang
University of Washington

Wenjing Zhou
University of Michigan

Kevin Jamieson
University of Washington

Simon Shaolei Du
University of Washington

Abstract

Data selection has emerged as a core issue for large-scale visual-language model pretraining (e.g., CLIP), particularly with noisy web-curated datasets. Three main data selection approaches are: (1) leveraging external non-CLIP models to aid data selection, (2) training new CLIP-style embedding models that are more effective at selecting high-quality data than the original OpenAI CLIP model, and (3) designing better metrics or strategies universally applicable to any CLIP embedding without requiring specific model properties (e.g., CLIPScore is one popular metric). While the first two approaches have been extensively studied, the third remains under-explored. In this paper, we advance the third approach by proposing two new methods. Firstly, instead of classical CLIP scores that only consider the alignment between two modalities from a single sample, we introduce **negCLIPLoss**, a CLIP loss-inspired method that adds the alignment between one sample and its contrastive pairs as an extra normalization term for better quality measurement. Secondly, when downstream tasks are known, we propose a new norm-based metric, **NormSim**, to measure the similarity between pretraining data and target data. We test our methods on the data selection benchmark, DataComp [1]. Compared to the best baseline using only OpenAI’s CLIP-L/14, our methods achieve a 5.3% improvement on ImageNet-1k and a 2.8% improvement on 38 downstream evaluation tasks. Moreover, both **negCLIPLoss** and **NormSim** are compatible with existing techniques. By combining our methods with the current best methods DFN [2] and HYPE [3], we can boost average performance on downstream tasks by 0.9%, achieving a new state-of-the-art.

1 Introduction

Curating large-scale visual-language datasets from web-sourced data has become common for pretraining multi-modal models. However, the quality of these web-curated data pairs remains a critical bottleneck. Research has shown that the choice of dataset significantly impacts model performance, irrespective of the models and training techniques employed [4–7], and this motivates the development of various data selection strategies. This paper focuses on optimizing subset selection from a fixed data pool to train a CLIP model [4] that achieves superior performance on zero-shot downstream tasks.

*Equal contribution. Correspondence to ypwang61@cs.washington.edu.

Classical methods *rely solely on OpenAI’s (OAI) pretrained CLIP model* (i.e., a teacher model) and focus on better utilizing the embeddings. The most commonly used one is calculating CLIPScore, which measures the cosine similarity between the visual and language embeddings of the CLIP model for the same sample, to eliminate low-quality data with mismatches between text and image. Other works also leverage heuristic distribution alignment techniques to select samples relevant to downstream tasks, such as image-based filtering [1]. These approaches are generally viewed as providing only limited enhancements. However, we argue that the potential of those embeddings has been heavily under-explored. This work seeks a universal method to better employ any given embeddings, not only from OAI CLIP, but also from other CLIP-style models.

On the other hand, recent leading data filtering methods, instead of focusing on improving embedding utilization strategy itself, mainly follow the other two directions, both employing external resources. They either (1) use *external non-CLIP models* that aid in data selection, (2) or use *external high-quality multi-modal data* to train a *better CLIP-style embedding model* than the original OAI CLIP to filter out low-quality data. Specifically, in the first line of works, HYPE [3] leverages embeddings from hyperbolic models instead of the classical Euclidean-based CLIP to measure how each data point has semantically overlaps with other data points and filters out data with low specificity. T-MARS [8] removes images where the text is the only feature correlated with the caption using FAST [9], an off-the-shelf OCR text detection model. Devil [10] applies fasttext [11] to remove non-English texts and use BLIP-2 [12] model for digit recognition to keep useful images with digits. The second direction, represented by Data Filtering Network (DFN) [2], involves training a new CLIP-style teacher model that uses high-quality datasets like HQITP-350M. Although the embeddings extracted from this model perform worse than the OAI CLIP in downstream tasks, it is particularly good at filtering out low-quality data. Notably, some of these methods can be combined and indeed, merging the selected data from DFN and HYPE achieves current state-of-art as shown in HYPE paper [3].

Previous works mainly focus on improving the CLIP embedding quality or utilizing an external model to do filtering but employ the CLIP embedding in a suboptimal way by only using classical methods like CLIPScore. In contrast, in this work, we focus on improving the filtering methods themselves for any given CLIP embedding. We show that there are universal and more effective strategies for utilizing any CLIP teacher model, regardless of its architecture (e.g., B/32 or L/14) or the dataset it was trained on (e.g., OpenAI-WIT-400M or DFN’s high-quality dataset). These strategies should always be orthogonal to the use of any newly trained CLIP-style models like DFN and might also be compatible with methods using external models like FAST and BLIP-2.

Our Contributions. We propose an alternative to CLIPScores that we call **negCLIPLoss** that more accurately characterizes data quality. We also introduce a new distribution metric we call the p-Norm Similarity Score (**NormSim**) when knowledge about downstream tasks is available. Two major observations directly inform our proposals:

- Firstly, we observe that classical methods measure the quality of a multi-modal sample by computing the cosine similarity between its visual and language embeddings, believing that lower similarity indicates that the text does not match its image part well. However, we find that some less informative samples may have a systematic bias, which leads to higher CLIPScores. For example, the language part containing the word "image" can result in higher similarity with any visual part, even when the text does not accurately describe its image content. Our proposed method **negCLIPLoss**, inspired by the standard CLIPLoss, normalizes the original CLIPScore by the similarity between a sample and its contrastive pairs. For example, the high score caused by the word "image" is typically consistent across its contrastive pairs, so our adjustment reduces this bias. As we have highlighted, such replacement can be universally applied across different embedding models. See Fig. 2 for illustrations.
- Secondly, if one has access to examples drawn from the same distribution as the target task, it is natural to assume that this extra knowledge could be leveraged to inform the data filtering process. We propose the **NormSim** metric to measure the vision similarity between a training sample x and the target task dataset $X_{\text{target}}^v \in \mathbb{R}^{n \times D}$ defined as $\|f_v(X_{\text{target}}^v)f_v(x^v)\|_p$, where $f_v : \mathbb{R}^D \rightarrow \mathbb{R}^d$ is the vision encoder of teacher model so that $f_v(X_{\text{target}}^v) \in \mathbb{R}^{n \times d}$, $f_v(x^v) \in \mathbb{R}^d$, and $f_v(X_{\text{target}}^v)f_v(x^v) \in \mathbb{R}^n$, and $\|\cdot\|_p$ is the p norm; effective choices are $p = 2$ or ∞ . Notably, unlike previous ImageNet-based filtering [1], which tries to keep the training set as diverse as downstream tasks by clustering the training set and finding the nearest neighbor group for *every target sample*, our method does not explicitly consider the diversity but greedily select examples as

long as it is close to *any target sample* (i.e. select high NormSimscore). Notably, **negCLIPLoss** and **NormSim** enjoy complementary effect in data selection. See Fig. 3.

To illustrate the effectiveness of our methods, we use a widely used benchmark DataComp [1] as our primary method of evaluating the datasets created by our data filtering methods. We show that, by simply replacing the CLIPScores with **negCLIPLoss** and utilizing **NormSim** we are able to exceed the best OAI-CLIP(L/14)-based baseline by 5.3% on ImageNet-1k and 2.8% on average across 38 downstream tasks, which is similar or even better than the performance achieved by many external-resources-based methods. Notably, even if the target downstream tasks are not available, we demonstrate that using NormSim on a proxy downstream task constructed from the training set, called **NormSim_{2-D}**, combined with negCLIPLoss, can also gain a 1.9% improvement on 38 downstream evaluation.

Moreover, the improvements achieved by our methods are not limited to OAI CLIP-based methods but can also be obtained by combining our methods with advanced models that require external resources. *By merging the subset selected by **negCLIPLoss** and **NormSim** with the subset selected by current state-of-the-art method “HYPER \cup DFN”, we can further improve it by 0.9% on both ImageNet-1k and on average 38 downstream tasks. Besides, we can also achieve a 0.8% improvement on average 38 tasks over “HYPER \cup DFN” using only the data selected by DFN and our strategies.* More importantly, we demonstrate that negCLIPLoss, as a replacement for CLIPScore, can be applied to any other embedding models like OAI-L/14, OAI-B/32, and DFN-B/32, universally boosting performance from 0.4% to 3.0% on an average of 38 tasks. This result is not only technically insightful for understanding the information available in embeddings but also practically significant. Compared to existing methods, our approach saves a significant amount of computational time on both reprocessing and new embedding retraining as shown in Table 4.

2 Problem Setup

Data Filtering on Multimodal Dataset. We are given a training dataset $D_{\text{train}} = \{x^v, x^l\}$, where $(x^v, x^l) \in \mathbb{R}^D$ is the image-text (vision-language) training pair. For convenience, we will let superscript vl denote either modality so that, for example, $x^{vl} \in x^v, x^l$. Our goal is to identify a subset $S \subset D_{\text{train}}$ that maximizes the zero-shot accuracy of the CLIP model on some downstream tasks when S is used to train the CLIP model.

CLIP score and embedding. Recent efforts, such as LAION [5] and DataComp [1], use OpenAI’s CLIP ViT-L/14 model [4] as a teacher model to obtain quality score. Here we denote this vanilla CLIP model as f_{vl} . For any pair x^{vl} , the model outputs a normalized unit-vector $\bar{f}_{vl}(x^{vl})$. If $X^{vl} := \{x_1^{vl}, \dots, x_m^{vl}\}$ denotes a dataset containing m samples, then we define $\bar{f}_{vl}(X^{vl}) = [\bar{f}_{vl}(x_1^{vl}), \dots, \bar{f}_{vl}(x_m^{vl})]^\top \in \mathbb{R}^{m \times d}$ as the embedding matrix. The popular filtering metric “CLIPScore” is defined as $\langle \bar{f}_v(x^v), \bar{f}_l(x^l) \rangle \in [-1, 1]$.

Dataset and model. Here we follow the pipeline of DataComp [1] to standardize the training and evaluation process. This is a testbed for dataset experiments aiming to open-source and further improve the vanilla CLIP model and is widely adopted in previous data selection papers [13, 14, 8, 2, 15, 7]. We will give more details in Sec. 4.

3 Data Filtering Strategy

3.1 negCLIPLoss: A Better Metric than CLIPScore

In this section, we introduce a better and statistically interpretable quality metric called negCLIPLoss, which directly replaces the common metric CLIPScore. Fig. 1 illustrates how negCLIPLoss works. This new metric only requires negligible extra computational costs and no additional external data collection costs. As the name suggested, this metric is inspired by the standard CLIP loss used in the actual training process of the teacher CLIP model, which is defined as

$$\ell_{B^*}(x_i^{vl}) = -\frac{1}{2} \left[\log \frac{\exp(\bar{f}_v(x_i^v)^\top \bar{f}_l(x_i^l)/\tau)}{\sum_{j \in B^*} \exp(\bar{f}_v(x_i^v)^\top \bar{f}_l(x_j^l)/\tau)} + \log \frac{\exp(\bar{f}_v(x_i^v)^\top \bar{f}_l(x_i^l)/\tau)}{\sum_{j \in B^*} \exp(\bar{f}_v(x_j^v)^\top \bar{f}_l(x_i^l)/\tau)} \right] \quad (1)$$

Here B^* is the random batch where i -th sample belongs during a particular training step, and τ is the learnable temperate parameter. Notably, the teacher loss differs from CLIPScore primarily by a

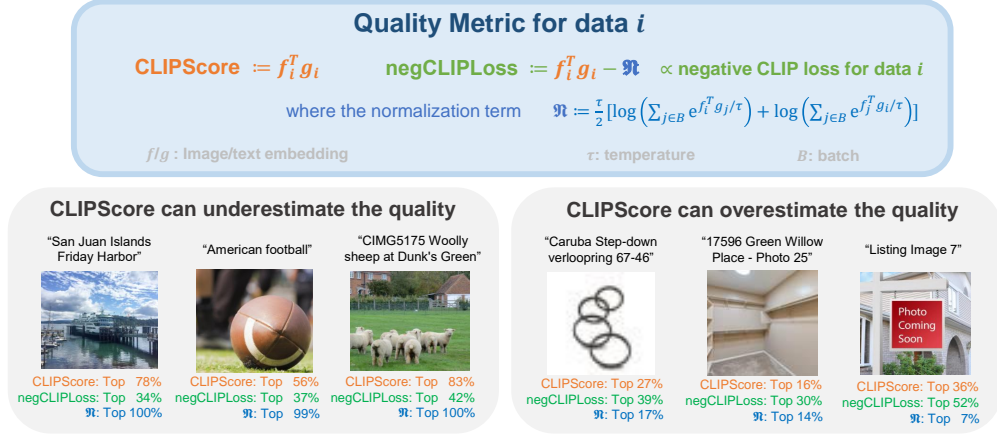


Figure 1: Illustration of negCLIPLoss. CLIPScore may underestimate (bottom left) or overestimate (bottom right) the quality of image-text pairs. However, this issue can be mitigated by simply adding a normalization term. negCLIPLoss employs the teacher model to calculate the negative CLIP loss on training data and serves as a more accurate metric. Here, “Top X%” denotes that the score represents the top X% *high* values within the entire dataset.

normalization term \mathcal{R}^* as follows:

$$-\tau \cdot \ell_{B^*}(x_i^{vl}) = \underbrace{\bar{f}_v(x_i^v)^\top \bar{f}_t(x_i^t)}_{\text{CLIPScore}} - \underbrace{\frac{\tau}{2} \left[\log \sum_{j \in B^*} \exp\left(\frac{\bar{f}_v(x_i^v)^\top \bar{f}_t(x_j^t)}{\tau}\right) + \log \sum_{j \in B^*} \exp\left(\frac{\bar{f}_v(x_j^v)^\top \bar{f}_t(x_i^t)}{\tau}\right) \right]}_{\text{normalization term } \mathcal{R}^*}$$

In practice, since the training dataset of teacher CLIP models, like OAI-WIT400M [4], and the actual batch divisions B^* is inaccessible, we randomly select K batches from the student model’s training data and use the averaged results from $\{B_k\}_{k=1}^K$ to estimate the normalization term \mathcal{R}^* on B^* , as shown in Eqn. 2:

$$\text{negCLIPLoss}(x_i^{vl}) := -\frac{\tau}{K} \sum_{k=1}^K \ell_{B_k}(x_i^{vl}) \approx \text{CLIPScore}(x_i^{vl}) - \mathcal{R}^* \quad (2)$$

Here $\{B_k\}_{k=1}^K$ are some batches randomly selected from the student model’s training data and $x_i \in B_k, \forall k$. We choose $K = 10$ in our experiments, but any sample size larger than 5 is sufficiently stable for estimating the original CLIPLoss (Details in Appendix D.1). Besides, in Sec. 4.3.3 we also show that the computational cost introduced by \mathcal{R} remains negligible compared to other baselines. The temperature τ and batch size $|B^*|$ can be directly obtained from the parameters of the pretrained teacher model, and the algorithm process of calculating negCLIPLoss is in Appendix C.2.

Motivation behind negCLIPLoss. Other existing works also use loss-guided data selection, such as LESS [16] in NLP, CoDis [17] in CV, and RHO [18] in general data scheduling scenarios. However, it is still unclear whether selecting based on teacher loss is suitable for multi-modal contrastive learning. Here we give an affirmative answer as shown in Fig. 2, where we can see negCLIPLoss performs better than or on par with CLIPScore consistently.

To illustrate how teacher loss helps our selection, we demonstrate that the normalization term provided by negCLIPLoss is crucial for correcting the overestimation or underestimation inherent in CLIPScore. A high normalization term implies that either the image embedding, text embedding, or both can easily match multiple contrastive pairs beyond their corresponding counterparts. For example, in the bottom right of Fig. 1, the text containing “Image” or “Photo” can be easily matched with any visual content. Similarly, the image of “verlooping” only contains very simple features and can be matched with many words like “white”, “empty” or “circle”,

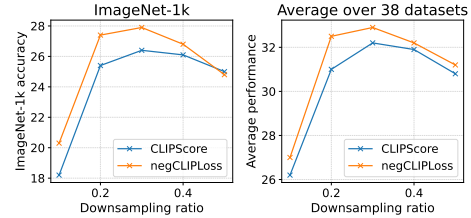


Figure 2: Comparison of negCLIPLoss and CLIPScore across different downsampling ratios on DataComp-medium.

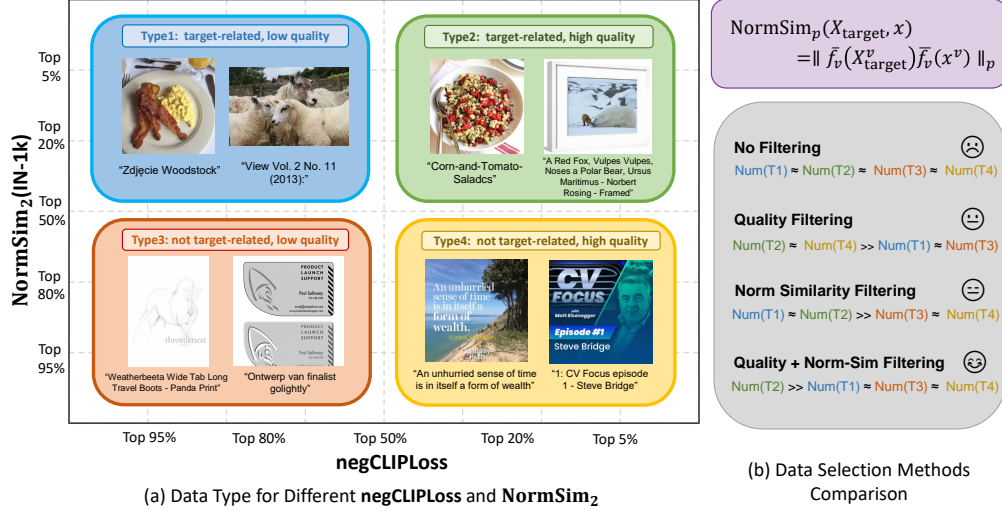


Figure 3: Illustration of NormSim on DataComp. X_{target} is the target prior data. “Top X%” denotes that the score represents the top X% high values within the entire dataset. (a) Visualization of data with different NormSim and negCLIPLoss. Here we use NormSim₂(ImageNet-1k) as an example. Although both Type 2 and Type 4 data have high negCLIPLoss and thus high quality, data with low NormSim₂ (Type 4) are more irrelevant to downstream tasks like ImageNet, VTAB, and MSCOCO. For example, they contain many images dominated by OCR content and make little contribution to improving downstream performance. (b) Illustration of a rough comparison of sampling data for different filtering methods. Using “negCLIPLoss \cap NormSim” filtering can balance the quality and relevance to downstream tasks, thus increasing the proportion of Type 2 data. (Refer to Appendix E for more visualization.)

etc. Consequently, despite a high absolute CLIPScore, the relative negCLIPLoss within its batch can be lower. In contrast, the bottom left features highly specific elements in both text and images, such as “Islands Harbor,” “American football”, and “sheep at green”. These elements are specific and less likely to match with contrastive pairs, resulting in a higher relative negCLIPLoss.

3.2 NormSim: A New Training-Target Similarity Metric

Our proposed negCLIPLoss is a universal approach to improve filtering performance by estimating quality better, and it does not rely on any downstream task. Now, if we can access some knowledge of the downstream tasks, we could further improve the performance by using a vision-only p -norm similarity to target data metric to measure the relationship between each training sample and the downstream target data. We will discuss the reason to use vision-only embedding later in this section.

Specifically, we assume access to the target set of downstream tasks and denote them as $X_{\text{target}} = \{x_{\text{target},(1)}, \dots, x_{\text{target},(m)}\}$, where each $x_{\text{target},(i)} \in \mathbb{R}^d$ is *i.i.d.*-sampled from the target downstream distribution $\mathcal{P}_{\text{target}}$ ², but without overlapping with the test set. Then, for each training sample x^{vl} and the corresponding target set X_{target} , the NormSim is defined as:

$$\text{NormSim}_p(X_{\text{target}}, x) := \|\bar{f}_v(X_{\text{target}}^v) \bar{f}_v(x^v)\|_p = \left(\sum_{x_t \in X_{\text{target}}} |\langle \bar{f}_v(x_t^v), \bar{f}_v(x^v) \rangle|^p \right)^{1/p} \quad (3)$$

We select the subset S of size N by greedily choosing the samples with the largest NormSim scores. The choice of the norm type p can be based on the data distribution and training process. In this paper, we consider two instantiations of p :

When $p = 2$, this data selection method is equivalent to selecting a subset that aligns with the principal components of the target set variance. In other words, it can be regarded as

$$S = \arg \max_{|S|=N} \sum_{i \in S} \bar{f}_v(x_i^v)^\top \left(\frac{1}{|X_{\text{target}}|} \sum_{x_t \in X_{\text{target}}} \bar{f}_v(x_t^v) \bar{f}_v(x_t^v)^\top \right) \bar{f}_v(x_i^v) \quad (4)$$

²Although out-of-distribution tasks like “WILDS” have distribution shift between training data and test data, they still provides useful information of the test data.

When $p = \infty$, the distance metric can be regarded as an even more optimistic measure, such that a training sample will be selected if it has high similarity to *any target sample*. Note that this is different from nearest-neighbor-based method used in image-based filtering [1], where they are trying to find the nearest training sample of *every target sample*. In this case, it can be regarded as:

$$S = \arg \max_{|S|=N} \sum_{i \in S} \max_{x_t \in X_{\text{target}}} \bar{f}_v(x_t^v)^\top \bar{f}_v(x_i^v) \quad (5)$$

In Appendix D.3, we also show that our NormSim $_{\infty}$ can outperform the nearest neighbor selection on the downstream target tasks. Here, we show an example selected via the NormSim $_2$ (ImageNet-1k) in Fig. 3, showing that this vision-target-aware method is complementary to the quality-based one.

Choice of Target Data. In the experiment parts, we try two kinds of target data: training data from ImageNet-1k (1.3M) or training data from all 24 accessible downstream tasks (2.1M)³. We denote them as NormSim $_p$ (IN-1k) and NormSim $_p$ (Target), respectively.

Necessity of using vision-only information. We use only the visual information x^v instead of multi-modal information x^{vl} for measuring similarity. This is because common crawled text often has brief captions, making the OAI CLIP language embedding weaker than its visual embedding model [1, 19–21]. Consequently, the language part cannot characterize the pre-training and downstream task distribution as well as the visual part. This phenomenon is also observed in Gadre et al. [1], where image-based filtering (select data whose image embeddings are similar to that from ImageNet-1k) outperforms text-based filtering (select data whose captions contain words from ImageNet-21k). More ablation studies are provided in Appendix D.4.

Using proxy when downstream X_{target} is inaccessible. Surprisingly, we show that the 2-norm can also be used when only the pre-training set is available. In this case, we construct a proxy “target” set from the pre-training set itself. Specifically, let S_i be the selected subset at step i , then we treat the current S_i as the proxy “target” set. To construct the next smaller set, we greedily select the next data batch S_{i+1} satisfying $\arg \max_{S_{i+1} \subset S_i} \sum_{x \in S} \text{NormSim}_2(S_i, x)$, until reaching an N size subset. We call this approach NormSim $_2$ -D (Dynamic) and will specify the algorithm details in Appendix C.3.

Theoretical justification. Unlike many existing methods that force diversity by selecting training samples around each x_{target} , our strategy greedily maximizes similarity without considering actual coverage. For the $p = 2$ case, we demonstrate that maximizing NormSim $_2$ is optimal under a linear model \bar{f}_v , as shown in Appendix A. Our theorem also provides error guarantees for noisy embeddings and explains when vision-only embeddings outperform combined vision and language embeddings. Recent work by Joshi et al. [22] provides a similar analysis but focuses on high-quality data and cross-variance between images and texts. This approach is less effective than image-only methods for filtering noisy datasets, as discussed above.

4 Experimental Results

In this section, we evaluate the performance of negCLIPLoss and NormSim, aiming to address the following questions: **Q1:** Given a fixed CLIP teacher model, can our methods more effectively utilize CLIP embeddings for data filtering? **Q2:** Are our methods applicable to diverse CLIP teacher models with varying architectures or different pretrained datasets? **Q3:** How does our method compare to other leading approaches that utilize external models or multimodal datasets? Additionally, could our method be compatible with these methods and enhance their effectiveness?

4.1 Setup

We adhere to the standardized training and evaluation protocols of the DataComp benchmark [1].

Training configuration. We employ the medium-scale training configuration of DataComp (DataComp-medium). It provides a substantial dataset comprising 128 million low-quality, web-curated image-text pairs to be filtered. Once the data subset is obtained by some data filtering strategy, it will be used to train a fixed CLIP-B/32 model in a fixed training budget that allows the model to pass 128 million data points an epoch. Therefore, smaller subsets will be repeated more frequently, ensuring a fair comparison. We note that the size of the DataComp dataset becomes smaller over time since some URLs of images become invalid⁴, and we only successfully downloaded about 110M data.

³Here we only use the target data for data selection, instead of training on them. The target dataset is significantly smaller than pretraining set like DataComp-medium (128M) or external datasets like HQITP-350M utilized by DFN [2].

⁴See <https://github.com/mlfoundations/datacomp/issues/3>. Similar issues are proposed by \mathbb{D}^2 pruning [14].

Therefore, the results of baselines on the leaderboard do not apply to our datasets, and we reproduce all the top baselines on the leaderboard with their public UIDs of the selected data.

Evaluation. We measured the model performance on 38 downstream datasets including image classification and retrieval tasks followed by DataComp. The image classification tasks contain ImageNet-1k [23], ImageNet distribution shifts [24–27], 11 datasets from the Visual Task Adaptation Benchmark (VTAB) [28] and 3 datasets from WILDS [29, 30]. Retrieval datasets contain Flickr30k [31], MSCOCO [32] and WinoGAViL [33].

Teacher model architecture. Our experiments utilize two architectures for OpenAI’s CLIP teacher models: ViT-L/14 and ViT-B/32. Additionally, we use the public version of DFN (DFN-P) proposed by Fang et al. [2] as a teacher model, and its architecture is also ViT-B/32.

4.2 Baselines

We restate the three current research directions mentioned before based on how much external resources are employed: (D1) using OAI CLIP alone while optimizing embedding employment strategies, (D2) training and using a more advanced CLIP embedding model based on external data, and (D3) utilizing non-CLIP external models to aid data selection. It is important to note that D2 and D3 may also incorporate strategies from D1. For example, CLIPScore (D1) has been used in almost all the top methods. Therefore, we categorize baselines by the largest possible category they encompass. According to the above categorization, we summarize the baselines we used in our experiments as follows. Please refer to Fig. 4 and Appendix C.4 for more details.

D1: OAI CLIP embedding only. The learner can only access the pretraining dataset (like DataComp-medium), the original OAI CLIP teacher model that is used to extract embeddings, and some target data of the downstream tasks which is much smaller than the pretraining dataset (like ImageNet-1k). In this category, we don’t use any existing external non-CLIP models or any newly trained CLIP model based on external multi-modal dataset. In detail, This category includes (1) **CLIPScore** [34], which only uses CLIPScore for filtering as we mentioned before. (2) **Image-based filtering** [1], which uses ImageNet-1K training data as the downstream target data for data filtering. It applies k-means clustering to the *image* embeddings of training data and selects clusters closest to the ImageNet-1K embeddings. Gadre et al. [1] also try to combine image-based filtering and CLIPScore together. (3) \mathbb{D}^2 **Pruning** [14], which represents the dataset as an undirected graph and selects the data by combining difficulty and diversity. They use the CLIP score to initialize their graph.

D2, D3: Accessible external model and multi-modal data. All the current top baselines enable the learner to utilize external resources, either to train a better CLIP teacher model or to help filtering using existing models’ properties. In detail, (1) **DFN** [2] trains another CLIP data filtering network via external high-quality data. Their currently public model (**DFN-P**) is trained on CC12M [35] + CC3M [36] + SS15M [37], while the best DFN is trained on nonpublic HQITP-350M [2], which is even larger than DataComp-medium. (2) **HYPE** [3] leverages hyperbolic embeddings (different from CLIP embedding) and the concept of entailment cones to filter out samples with meaningless or underspecified semantics, enhancing the specificity of each sample. (3) **HYPE** \cup **DFN** proposed by [3] samples subset separately for each method and then merge them. This is the state-of-the-art method on the DataComp benchmark for medium size. (4) Other methods including **T-MARS** [8], **Devils** [10], **MLM** [38], which leverage external models such as text detection model FAST [9], vision-language model (VLM) BLIP-2 [12] and VLM LLaVA-1.5 [39, 40] to heuristically select the more helpful data, like non-text-only pictures or images with MNIST-style digits. See details in Appendix C.4.

Cross-setting comparison. We make these separations for fair comparison. Intuitively, performance should be ranked as **D2, D3** > **D1**. However, our results show that cross-setting comparisons are possible and our D1 methods can perform similar or even better than most of D3 methods.

4.3 Main Results and Discussions

4.3.1 Comparison on D1 Category (Q1)

In Table 1, we compare the D1 methods where only the OAI CLIP model is allowed to be used.

Our Methods leverage OAI CLIP-L/14 better. *First*, negCLIPLoss outperforms CLIPScore on *all metrics*, regardless of whether it is used alone or combined with other methods. These results support our claim that negCLIPLoss can more accurately estimate the data quality.

Table 1: Results on DataComp-medium from methods that use only OpenAI’s CLIP-L/14 model, i.e., all methods are from the **D1** category. The “dataset size” represents the size of the subset obtained from different approaches. NormSim(IN-1k) denotes using the training data of ImageNet-1k as the target while NormSim(Target) represents using that of all 24 available downstream tasks. NormSim-D refers to the methods that use an iteratively selected subset from the training set as the target proxy.

Filtering Strategy	Dataset Size	IN-1k (1 task)	IN Dist. Shift (5)	VTAB (11)	Retrieval (3)	Avg. (38)
No filtering [1]	110M	17.3	15.0	25.2	21.3	25.6
CLIPScore (20%) [34]	22M	25.4	22.7	31.8	22.0	31.0
CLIPScore (30%) [34]	33M	26.4	23.6	32.6	24.5	32.2
Image-based [1]	24M	25.5	21.9	30.4	24.6	29.9
CLIPScore (30%) \cap Image-based [1]	11M	27.4	23.9	31.9	21.4	30.8
\mathbb{D}^2 Pruning [14]	22M	23.2	20.4	31.4	18.7	29.5
negCLIPLoss (20%)	22M	27.4	23.8	33.7	23.7	32.5
negCLIPLoss (30%)	33M	27.9	24.6	33.2	25.1	32.9
CLIPScore (30%) \cap NormSim ₂ -D	22M	28.3	25.0	34.5	22.7	32.9
negCLIPLoss (30%) \cap NormSim ₂ -D	22M	29.8	26.1	34.8	24.6	34.1
CLIPScore (30%) \cap NormSim ₂ (IN-1k)	22M	29.1	25.4	<u>35.8</u>	24.1	33.4
CLIPScore (30%) \cap NormSim ₂ (Target)	22M	28.9	25.1	32.7	23.6	32.5
CLIPScore (30%) \cap NormSim _{∞} (IN-1k)	22M	29.7	25.9	33.7	24.1	33.7
CLIPScore (30%) \cap NormSim _{∞} (Target)	22M	30.2	26.2	35.0	23.4	33.9
negCLIPLoss (30%) \cap NormSim ₂ (IN-1k)	22M	30.4	26.4	35.4	25.6	34.3
negCLIPLoss (30%) \cap NormSim ₂ (Target)	22M	30.6	26.2	35.2	25.5	33.9
negCLIPLoss (30%) \cap NormSim _{∞} (IN-1k)	22M	31.9	27.3	34.8	25.0	<u>34.4</u>
negCLIPLoss (30%) \cap NormSim _{∞} (Target)	22M	<u>31.7</u>	<u>27.2</u>	36.0	26.0	35.0

Second, even when target knowledge is unavailable, use NormSim₂-D together with negCLIPLoss can still improve the filtering performance by 1.9% on average 38 downstream tasks. *Third*, when target knowledge is available, NormSim₂ and NormSim _{∞} can improve filtering more significantly compared with NormSim₂-D, and *in general*, NormSim _{∞} is the best choice. Especially, compared with the best baseline ‘CLIPScore (30%)’, our best combination ‘negCLIPLoss \cap NormSim _{∞} (Target)’ improves **5.3%** on **ImageNet-1k** and **2.8%** on average **38 downstream tasks**, respectively. Later in Table 3 we will see that this result outperform all the D3 baselines except DFN \cup HYPE. On the other hand, when using ImageNet-1k as the target data, the choice of norm has very little influence.

4.3.2 Try Other Teacher Models (Q2)

To evaluate whether our method applies to other CLIP teacher models, we replaced OAI CLIP-L/14 with OAI CLIP-B/32 and DFN-P as embedding models. We compare the best baseline “CLIPScore” with our “negCLIPLoss” and best strategy “negCLIPLoss \cap NormSim _{∞} (Target)” as shown in Table 2 and Appendix D.2. Note that the original DFN paper selects a subset comprising 19.2M data points, which accounts for approximately 17.5% of our dataset and 15% of their dataset, we incorporate these sampling ratios into our comparison.

Table 2: Results on DataComp-medium from the top methods that use only OpenAI’s CLIP-B/32 model or public version of DFN (DFN-P). “NormSim _{∞} ^{B/32}” represents using OAI CLIP-B/32 to calculate NormSim _{∞} .

Strategy	Size	IN-1k	VTAB	Avg.
OAI CLIP-B/32				
CLIPScore (20%)	22M	27.0	33.0	32.2
CLIPScore (30%)	33M	27.6	33.6	33.2
negCLIPLoss (20%)	22M	28.9	34.3	33.0
negCLIPLoss (30%)	33M	28.8	33.7	33.6
negCLIPLoss (30%) \cap NormSim _{∞} (Target)	22M	32.4	35.9	35.2
DFN-P				
CLIPScore (15%)	16M	25.9	32.9	31.6
CLIPScore (17.5%)	19M	30.2	34.1	33.8
CLIPScore (20%)	22M	29.7	33.0	33.1
CLIPScore (30%)	33M	28.4	33.2	32.7
negCLIPLoss (15%)	16M	31.3	35.8	34.6
negCLIPLoss (17.5%)	19M	31.2	35.7	<u>34.7</u>
negCLIPLoss (20%)	22M	30.7	33.6	33.8
negCLIPLoss (30%)	33M	28.9	33.4	33.2
negCLIPLoss (30%) \cap NormSim _{∞} (Target)	22M	29.4	33.5	32.5
negCLIPLoss (17.5%) \cap NormSim _{∞} ^{B/32} (Target)	16M	31.6	37.2	35.7

Table 3: Results of all D1&D2&D3 top methods on DataComp-medium. The results of MLM [38] are from their paper, while all other baselines are reproduced on our downloaded dataset using their official UIDs. “Ours (20%)” refers to use “negCLIPLoss (30%) \cap NormSim $_{\infty}$ (Target)” to get 20% of original data, while “Ours (10%)” denotes applying “negCLIPLoss (20%) \cap NormSim $_{\infty}$ (Target)” to get 10%. And we use “*” to indicate the case where we choose the intersection of the data selected by using OAI CLIP-B/32 and OAI CLIP-L/14 separately, which results in about 15M data for “Ours (20%)*” and 7.4M data for “Ours (10%)*”.

Type	Filtering Strategy	Dataset Size	IN-1k (1)	IN Dist. Shift (5)	VTAB (11)	Retrieval (3)	Avg. (38)
D2	DFN [2]	16M	36.0	30.1	36.2	27.0	35.4
D3	T-MARS [8]	22M	30.8	26.3	34.8	25.4	34.1
D3	Devil [10]	20M	31.0	26.7	35.9	24.7	34.5
D3	MLM [38]	38M	30.3	25.6	36.0	29.0	34.5
D3	HYPE [3]	10M	30.3	25.8	34.3	22.2	31.9
D3	DFN \cup HYPE [3]	20M	<u>36.4</u>	30.8	<u>38.5</u>	28.0	36.8
D1	Ours (20%)	22M	32.4	27.4	35.9	26.3	35.2
D3	DFN \cup Ours (20%)*	23M	<u>36.4</u>	<u>30.9</u>	38.6	<u>28.1</u>	<u>37.6</u>
D3	DFN \cup HYPE \cup Ours (10%)*	22M	37.3	31.4	<u>38.5</u>	27.6	37.7

negCLIPLoss can be applied to different CLIP embedding models. Our proposed negCLIPLoss, as a replacement of CLIPScore, not only leads to better performance compared to all the other baselines using OAI CLIP-L/14 as shown in Table 1, but also achieves universal improvement on the other two CLIP embedding models, OAI CLIP-B/32 and DFN-P as shown in Table 2. Our methods can consistently outperform all downstream tasks for different filtering ratios and models, like a 0.5%-5.4% increase on ImageNet-1k.

Embedding required by NormSim should have good downstream performance. When combining negCLIPLoss with NormSim $_{\infty}$, OAI CLIP-B/32 and DFN-P exhibit completely different behaviors. The former obtains results even better than those in Table 1, which uses OAI CLIP-L/14 as the teacher model, while DFN-P achieves results even worse than using negCLIPLoss alone (see “negCLIPLoss (30%) \cap NormSim $_{\infty}$ (Target)” and “negCLIPLoss (20%)/(30%)”). The reason is that, unlike OAI CLIP-B/32, DFN-P is specially designed for data filtering *at the expense of downstream task performance*, as claimed by its authors. For example, the ImageNet-1k accuracy for DFN-P, OAI CLIP-B/32, and OAI CLIP-L/14 are 45%, 63%, and 75%, respectively. This indicates that the embeddings obtained from DFN on target data might be highly unreliable, leading to inaccurate similarity calculations between training and target data. To support this, if we use DFN-P to evaluate negCLIPLoss but utilize OAI CLIP-B/32 for calculating NormSim, as shown in “negCLIPLoss (17.5%) \cap NormSim $_{\infty}^{B/32}$ (Target)”, we can further improve the results compared to using negCLIPLoss alone. Its average performance on 38 tasks is even higher than utilizing the best DFN (trained on HQITP-350M) with CLIPScore, as shown in Table 3.

4.3.3 Comparison with D2 & D3 Categories (Q3)

In this part, we compare all the D2 & D3 baselines mentioned in Sec. 4.2 together with our best strategy in Table 3. Here we reproduce all the baselines if their official UIDs are available. For “A \cup B” mentioned in Table 3, we follow the way of “HYPE \cup DFN” in Kim et al. [3] to merge the data, which generates the sampling subset separately for each method and then merge them. This will result in oversampling the shared data, which is intuitively more important.⁵

Our methods can outperform most of the D3 methods. In Table 3, we show that without using any external models or data, our best combination, i.e., using OAI CLIP-B/32 for “negCLIPLoss (30%) \cap NormSim $_{\infty}$ (Target)” (**Ours (20%)**), still outperforms all methods except DFN and “DFN \cup HYPE”. This answers the first part of Q3 and further indicates that some external models may be redundant since CLIP embeddings already contain necessary information.

We can further improve the SOTA method. We show that our model can further boost the performance of the current SOTA method “HYPE \cup DFN” by 0.9% on both ImageNet-1k and on average 38 downstream tasks, and close results can be achieved even without combining HYPE which utilizes the external embedding model MERU [41]. Here we use the data selected by both OAI

⁵For the dataset size of “A \cup B”, we count the number of the unique data in the dataset followed HYPE [3].

CLIP-B/32 and L/14, which we found is more robust than using one of them alone. Our better results answer the second part of Q3, that is, our methods can be compatible with other D2&D3 methods.

5 Conclusion and Limitation

In this paper, we introduce two metrics, negCLIPLoss and NormSim, to enhance data selection in multimodal contrastive learning without relying on external resources. negCLIPLoss provides a more accurate quality metric compared to the commonly used CLIPScore, while NormSim measures the similarity between pretraining data and target data for known downstream tasks. Experiments show that our methods achieve results that are competitive with or even better to approaches using external models or datasets. Additionally, negCLIPLoss and NormSim are compatible with existing top techniques, allowing us to achieve a new state-of-the-art by combining them.

A notable limitation of our study is the exclusion of larger pretraining datasets, such as the large and xlarge scales of DataComp. However, DataComp-medium is the most commonly used benchmark for data selection in CLIP pretraining, and our method has demonstrated both effectiveness (Table 1-3) and efficiency (Table 4) on it. Future directions include exploring better ways to merge data selected by different methods and incorporating our methods into data scheduling scenarios.

References

- [1] Samir Yitzhak Gadre, Gabriel Ilharco, Alex Fang, Jonathan Hayase, Georgios Smyrnis, Thao Nguyen, Ryan Marten, Mitchell Wortsman, Dhruva Ghosh, Jieyu Zhang, et al. Datacomp: In search of the next generation of multimodal datasets. *arXiv preprint arXiv:2304.14108*, 2023.
- [2] Alex Fang, Albin Madappally Jose, Amit Jain, Ludwig Schmidt, Alexander Toshev, and Vaishaal Shankar. Data filtering networks. *arXiv preprint arXiv:2309.17425*, 2023.
- [3] Wonjae Kim, Sanghyuk Chun, Taekyung Kim, Dongyoon Han, and Sangdoo Yun. Hype: Hyperbolic entailment filtering for underspecified images and texts. *arXiv preprint arXiv:2404.17507*, 2024.
- [4] Alec Radford, Jong Wook Kim, Chris Hallacy, Aditya Ramesh, Gabriel Goh, Sandhini Agarwal, Girish Sastry, Amanda Askell, Pamela Mishkin, Jack Clark, et al. Learning transferable visual models from natural language supervision. In *International conference on machine learning*, pages 8748–8763. PMLR, 2021.
- [5] Christoph Schuhmann, Romain Beaumont, Richard Vencu, Cade Gordon, Ross Wightman, Mehdi Cherti, Theo Coombes, Aarush Katta, Clayton Mullis, Mitchell Wortsman, et al. Laion-5b: An open large-scale dataset for training next generation image-text models. *Advances in Neural Information Processing Systems*, 35:25278–25294, 2022.
- [6] Mehdi Cherti, Romain Beaumont, Ross Wightman, Mitchell Wortsman, Gabriel Ilharco, Cade Gordon, Christoph Schuhmann, Ludwig Schmidt, and Jenia Jitsev. Reproducible scaling laws for contrastive language-image learning. In *Proceedings of the IEEE/CVF Conference on Computer Vision and Pattern Recognition*, pages 2818–2829, 2023.
- [7] Jinze Bai, Shuai Bai, Shusheng Yang, Shijie Wang, Sinan Tan, Peng Wang, Junyang Lin, Chang Zhou, and Jingren Zhou. Qwen-vl: A frontier large vision-language model with versatile abilities. *arXiv preprint arXiv:2308.12966*, 2023.
- [8] Pratyush Maini, Sachin Goyal, Zachary C Lipton, J Zico Kolter, and Aditi Raghunathan. T-mars: Improving visual representations by circumventing text feature learning. *arXiv preprint arXiv:2307.03132*, 2023.
- [9] Zhe Chen, Jiahao Wang, Wenhai Wang, Guo Chen, Enze Xie, Ping Luo, and Tong Lu. Fast: Faster arbitrarily-shaped text detector with minimalist kernel representation, 2021.
- [10] Haichao Yu, Yu Tian, Sateesh Kumar, Linjie Yang, and Heng Wang. The devil is in the details: A deep dive into the rabbit hole of data filtering. *arXiv preprint arXiv:2309.15954*, 2023.
- [11] Armand Joulin, Edouard Grave, Piotr Bojanowski, and Tomas Mikolov. Bag of tricks for efficient text classification. *arXiv preprint arXiv:1607.01759*, 2016.

- [12] Junnan Li, Dongxu Li, Silvio Savarese, and Steven Hoi. Blip-2: Bootstrapping language-image pre-training with frozen image encoders and large language models. In *International conference on machine learning*, pages 19730–19742. PMLR, 2023.
- [13] Thao Nguyen, Samir Yitzhak Gadre, Gabriel Ilharco, Sewoong Oh, and Ludwig Schmidt. Improving multimodal datasets with image captioning. *arXiv preprint arXiv:2307.10350*, 2023.
- [14] Adyasha Maharana, Prateek Yadav, and Mohit Bansal. D2 pruning: Message passing for balancing diversity and difficulty in data pruning. *arXiv preprint arXiv:2310.07931*, 2023.
- [15] Anas Mahmoud, Mostafa Elhoushi, Amro Abbas, Yu Yang, Newsha Ardalani, Hugh Leather, and Ari Morcos. Sieve: Multimodal dataset pruning using image captioning models. *arXiv preprint arXiv:2310.02110*, 2023.
- [16] Mengzhou Xia, Sadhika Malladi, Suchin Gururangan, Sanjeev Arora, and Danqi Chen. Less: Selecting influential data for targeted instruction tuning. *arXiv preprint arXiv:2402.04333*, 2024.
- [17] Xiaobo Xia, Bo Han, Yibing Zhan, Jun Yu, Mingming Gong, Chen Gong, and Tongliang Liu. Combating noisy labels with sample selection by mining high-discrepancy examples. In *Proceedings of the IEEE/CVF International Conference on Computer Vision (ICCV)*, pages 1833–1843, October 2023.
- [18] Sören Mindermann, Jan M Brauner, Muhammed T Razzak, Mrinank Sharma, Andreas Kirsch, Winnie Xu, Benedikt Hölten, Aidan N Gomez, Adrien Morisot, Sebastian Farquhar, and Yarin Gal. Prioritized training on points that are learnable, worth learning, and not yet learnt. In Kamalika Chaudhuri, Stefanie Jegelka, Le Song, Csaba Szepesvari, Gang Niu, and Sivan Sabato, editors, *Proceedings of the 39th International Conference on Machine Learning*, volume 162 of *Proceedings of Machine Learning Research*, pages 15630–15649. PMLR, 17–23 Jul 2022.
- [19] Sheng Shen, Liunian Harold Li, Hao Tan, Mohit Bansal, Anna Rohrbach, Kai-Wei Chang, Zhewei Yao, and Kurt Keutzer. How much can clip benefit vision-and-language tasks? *arXiv preprint arXiv:2107.06383*, 2021.
- [20] Yan Zeng, Xinsong Zhang, and Hang Li. Multi-grained vision language pre-training: Aligning texts with visual concepts. In *International Conference on Machine Learning*, pages 25994–26009. PMLR, 2022.
- [21] Yutaro Yamada, Yingtian Tang, and Ilker Yildirim. When are lemons purple? the concept association bias of clip. *arXiv preprint arXiv:2212.12043*, 2022.
- [22] Siddharth Joshi, Arnav Jain, Ali Payani, and Baharan Mirzasoleiman. Data-efficient contrastive language-image pretraining: Prioritizing data quality over quantity. In Sanjoy Dasgupta, Stephan Mandt, and Yingzhen Li, editors, *Proceedings of The 27th International Conference on Artificial Intelligence and Statistics*, volume 238 of *Proceedings of Machine Learning Research*, pages 1000–1008. PMLR, 02–04 May 2024.
- [23] Jia Deng, Wei Dong, Richard Socher, Li-Jia Li, Kai Li, and Li Fei-Fei. Imagenet: A large-scale hierarchical image database. In *2009 IEEE conference on computer vision and pattern recognition*, pages 248–255. Ieee, 2009.
- [24] Haohan Wang, Songwei Ge, Zachary Lipton, and Eric P Xing. Learning robust global representations by penalizing local predictive power. *Advances in Neural Information Processing Systems*, 32, 2019.
- [25] Benjamin Recht, Rebecca Roelofs, Ludwig Schmidt, and Vaishal Shankar. Do ImageNet classifiers generalize to ImageNet? In Kamalika Chaudhuri and Ruslan Salakhutdinov, editors, *Proceedings of the 36th International Conference on Machine Learning*, volume 97 of *Proceedings of Machine Learning Research*, pages 5389–5400. PMLR, 09–15 Jun 2019.
- [26] Dan Hendrycks, Kevin Zhao, Steven Basart, Jacob Steinhardt, and Dawn Song. Natural adversarial examples. In *Proceedings of the IEEE/CVF Conference on Computer Vision and Pattern Recognition*, pages 15262–15271, 2021.

- [27] Dan Hendrycks, Steven Basart, Norman Mu, Saurav Kadavath, Frank Wang, Evan Dorundo, Rahul Desai, Tyler Zhu, Samyak Parajuli, Mike Guo, et al. The many faces of robustness: A critical analysis of out-of-distribution generalization. In *Proceedings of the IEEE/CVF International Conference on Computer Vision*, pages 8340–8349, 2021.
- [28] Xiaohua Zhai, Joan Puigcerver, Alexander Kolesnikov, Pierre Ruyssen, Carlos Riquelme, Mario Lucic, Josip Djolonga, Andre Susano Pinto, Maxim Neumann, Alexey Dosovitskiy, et al. A large-scale study of representation learning with the visual task adaptation benchmark. *arXiv preprint arXiv:1910.04867*, 2019.
- [29] Pang Wei Koh, Shiori Sagawa, Henrik Marklund, Sang Michael Xie, Marvin Zhang, Akshay Balsubramani, Weihua Hu, Michihiro Yasunaga, Richard Lanus Phillips, Irena Gao, et al. Wilds: A benchmark of in-the-wild distribution shifts. In *International Conference on Machine Learning*, pages 5637–5664. PMLR, 2021.
- [30] Shiori Sagawa, Pang Wei Koh, Tony Lee, Irena Gao, Sang Michael Xie, Kendrick Shen, Ananya Kumar, Weihua Hu, Michihiro Yasunaga, Henrik Marklund, et al. Extending the wilds benchmark for unsupervised adaptation. *arXiv preprint arXiv:2112.05090*, 2021.
- [31] Peter Young, Alice Lai, Micah Hodosh, and Julia Hockenmaier. From image descriptions to visual denotations: New similarity metrics for semantic inference over event descriptions. *Transactions of the Association for Computational Linguistics*, 2:67–78, 2014.
- [32] Xinlei Chen, Hao Fang, Tsung-Yi Lin, Ramakrishna Vedantam, Saurabh Gupta, Piotr Dollár, and C Lawrence Zitnick. Microsoft coco captions: Data collection and evaluation server. *arXiv preprint arXiv:1504.00325*, 2015.
- [33] Yonatan Bitton, Nitzan Bitton Guetta, Ron Yosef, Yuval Elovici, Mohit Bansal, Gabriel Stanovsky, and Roy Schwartz. Winogavil: Gamified association benchmark to challenge vision-and-language models. *Advances in Neural Information Processing Systems*, 35:26549–26564, 2022.
- [34] Jack Hessel, Ari Holtzman, Maxwell Forbes, Ronan Le Bras, and Yejin Choi. Clipscore: A reference-free evaluation metric for image captioning. *arXiv preprint arXiv:2104.08718*, 2021.
- [35] Soravit Changpinyo, Piyush Sharma, Nan Ding, and Radu Soricut. Conceptual 12m: Pushing web-scale image-text pre-training to recognize long-tail visual concepts. In *Proceedings of the IEEE/CVF Conference on Computer Vision and Pattern Recognition*, pages 3558–3568, 2021.
- [36] Piyush Sharma, Nan Ding, Sebastian Goodman, and Radu Soricut. Conceptual captions: A cleaned, hypernymed, image alt-text dataset for automatic image captioning. In Iryna Gurevych and Yusuke Miyao, editors, *Proceedings of the 56th Annual Meeting of the Association for Computational Linguistics (Volume 1: Long Papers)*, pages 2556–2565, Melbourne, Australia, July 2018. Association for Computational Linguistics.
- [37] Thao Nguyen, Gabriel Ilharco, Mitchell Wortsman, Sewoong Oh, and Ludwig Schmidt. Quality not quantity: On the interaction between dataset design and robustness of clip. *Advances in Neural Information Processing Systems*, 35:21455–21469, 2022.
- [38] Weizhi Wang, Khalil Mrini, Linjie Yang, Sateesh Kumar, Yu Tian, Xifeng Yan, and Heng Wang. Finetuned multimodal language models are high-quality image-text data filters. *arXiv preprint arXiv:2403.02677*, 2024.
- [39] Haotian Liu, Chunyuan Li, Yuheng Li, and Yong Jae Lee. Improved baselines with visual instruction tuning. *arXiv preprint arXiv:2310.03744*, 2023.
- [40] Wei-Lin Chiang, Zhuohan Li, Zi Lin, Ying Sheng, Zhanghao Wu, Hao Zhang, Lianmin Zheng, Siyuan Zhuang, Yonghao Zhuang, Joseph E Gonzalez, et al. Vicuna: An open-source chatbot impressing gpt-4 with 90%* chatgpt quality. See <https://vicuna.lmsys.org> (accessed 14 April 2023), 2(3):6, 2023.
- [41] Karan Desai, Maximilian Nickel, Tanmay Rajpurohit, Justin Johnson, and Shanmukha Ramakrishna Vedantam. Hyperbolic image-text representations. In *International Conference on Machine Learning*, pages 7694–7731. PMLR, 2023.

- [42] Ryumei Nakada, Halil Ibrahim Gulluk, Zhun Deng, Wenlong Ji, James Zou, and Linjun Zhang. Understanding multimodal contrastive learning and incorporating unpaired data. In *International Conference on Artificial Intelligence and Statistics*, pages 4348–4380. PMLR, 2023.
- [43] Gene H Golub and Charles F Van Loan. *Matrix computations*. JHU press, 2013.
- [44] Martin J Wainwright. *High-dimensional statistics: A non-asymptotic viewpoint*, volume 48. Cambridge university press, 2019.
- [45] Jeff Johnson, Matthijs Douze, and Hervé Jégou. Billion-scale similarity search with gpus. *IEEE Transactions on Big Data*, 7(3):535–547, 2019.
- [46] Thao Nguyen, Samir Yitzhak Gadre, Gabriel Ilharco, Sewoong Oh, and Ludwig Schmidt. Improving multimodal datasets with image captioning. *Advances in Neural Information Processing Systems*, 36, 2024.
- [47] Sachin Goyal, Pratyush Maini, Zachary C Lipton, Aditi Raghunathan, and J Zico Kolter. Scaling laws for data filtering—data curation cannot be compute agnostic. *arXiv preprint arXiv:2404.07177*, 2024.

A Theoretical Interpretation

In this section, we give a theoretical justification on the NormSim metric when $p = 2$ under the linear model assumptions when low quality image and mismatched text has already been removed. In other words, we mainly focus on the following strategy.

$$S = \arg \max_{|S|=N} \sum_{i \in S} \bar{f}_v(x_i^v)^\top \underbrace{\left(\frac{1}{|X_{\text{target}}|} \sum_{x_t \in X_{\text{target}}} \bar{f}_v(x_t^v) \bar{f}_v(x_t^v)^\top \right)}_{\bar{\Sigma}_{\text{target_proxy}}} \bar{f}_v(x_i^v) \quad (6)$$

A.1 Theoretical Setup

Training data. For any $\mathbf{x}^v, \mathbf{x}^l \in \mathbb{R}^d$ observable image and text training pairs, we define $\mathbf{z}^v, \mathbf{z}^l$ to be the corresponding latent vectors which contain all semantically pertinent information about our tasks of interest. Similar to previous theoretical work [42], we assume each i.i.d pair \mathbf{z}^{vl} follows zero-mean sub-gaussian distribution whose cross-covariance satisfies

$$\text{Cov}(\mathbf{z}^v, \mathbf{z}^l) = \Sigma_{\text{train}} = \text{diag}(\sigma_1, \sigma_2, \dots), \quad \|\mathbf{z}^{vl}\| = 1$$

and each \mathbf{x}^{vl} is generated based on a linear model such that

$$\mathbf{x}^{vl} = G_{vl}^* \mathbf{z}^{vl} + \boldsymbol{\xi}^{vl}.$$

Here $G_{vl}^* \in O_{d \times r}$ is the orthonormal ground truth representation mapping from the latent vector space to the input space, and $\boldsymbol{\xi}^{vl} \sim \mathcal{N}(0, I_d)$ are i.i.d. random noise.

Also we denote the cross covariance of any finite dataset S' (e.g. the given train set D_{train}) as $\Sigma_{S'}$.

Test data. For any zero-shot downstream task, we assume it shares almost same data generation process as the training set, except its the cross-covariance Σ_{target} does not necessarily equal Σ_{train} , which necessitate the choice of $\bar{\Sigma}_{\text{target_proxy}}$.

CLIP embedding model as teacher. Under the linear model assumption, we have a teacher model $\bar{f}_{vl} = \bar{G}_{vl}$, whose generated clip embedding can partially recover the ground truth hidden vector \mathbf{z}^{vl} with error.

Formally, we say teacher has ϵ_v^n error if for all possible n budget subsets $S \subset D_{\text{train}}$,

$$\frac{1}{|S|} \left\| \sum_{\mathbf{x}^{vl} \in S} \bar{G}_v^\top \mathbf{x}^v (\mathbf{x}^v)^\top \bar{G}_v - \sum_{\mathbf{x}^{vl} \in S} \mathbf{z}^v (\mathbf{z}^v)^\top \right\|_* \leq \epsilon_v^n$$

where the same notation applies for the language modal. By the orthonormal assumption on the ground truth matrix G_{vl}^* , we see that \bar{G}_v^\top is aiming to inverting the map. In addition, we say the teacher has ϵ_{v*l}^n cross modal error

$$\frac{1}{|S|} \left\| \sum_{\mathbf{x}^{vl} \in S} \bar{G}_v^\top \mathbf{x}^v (\mathbf{x}^l)^\top \bar{G}_l - \sum_{\mathbf{x}^{vl} \in S} \mathbf{z}^v (\mathbf{z}^l)^\top \right\|_* \leq \epsilon_{v*l}^n$$

When all $\epsilon_v^n, \epsilon_l^n, \epsilon_{v*l}^n \rightarrow 0$ as $n \rightarrow \infty$, then we say the teacher is strong for both modalities. But it might also be possible that only one modal, for example, visual is strong. That is $\epsilon_v^n \rightarrow 0, \epsilon_l^n, \epsilon_{v*l}^n \gg \epsilon_v^n$.

Model and training. According to Lemma 4.1 in [42], using the CLIP loss to optimize the linear model has approximately the same training dynamics as using the regularized linear loss. Therefore, here we assume that we are learning G_v, G_l by maximizing the clip score gap between the contrastive pairs, plus a regularizer,

$$\min_{G_v, G_l} \mathcal{L}_S^\rho(G_v, G_l) := \min_{G_v, G_l} \frac{\sum_{i \in S} \sum_{j \in S} (s_{ij} - s_{ii})}{|S|(|S| - 1)} + \frac{\rho}{2} \frac{|S|}{|S| - 1} \|G_v G_l^\top\|_F^2$$

where $s_{ij} := \langle G_v^\top \mathbf{x}_i^v, G_l^\top \mathbf{x}_j^l \rangle$ and $\rho > 0$ is some regularizer-related *constant*. Note that this objective maximizes self-similarity and minimizes similarity between disparate pairs. Note that this “loss” can be negative, avoiding the trivial null solution of all zeros. We denote this training process from any given S as $G_{vl} = \mathcal{A}^\rho(S)$.

Goal and metric. Under the same principle as our training loss function, we measure the performance of any learnt G_v, G_l on some downstream task with distribution $\mathcal{D}_{\text{target}}$ as test loss $\mathcal{L}_{\text{target}}(G_v, G_l) :=$

$$\mathbb{E}_{\substack{\mathbf{x}^{vl} \sim \mathcal{D}_{\text{target}} \\ \mathbf{x}_2^{vl} \sim \mathcal{D}_{\text{target}}}} (\langle G_v^\top \mathbf{x}^v, G_l^\top \mathbf{x}_2^l \rangle - \langle G_v^\top \mathbf{x}^v, G_l^\top \mathbf{x}^l \rangle)$$

This is inspired by the following classification accuracy. Assume that the test data including C class, and the class distribution is \mathcal{C} . For every class c , the training data $\mathbf{x} = (\mathbf{x}^v, \mathbf{x}^l)$ satisfies distribution \mathcal{P}_c . We further assume the corresponding classification templates are $\{\mathbf{x}_c\}_{c=1}^C$. Thus we define classification accuracy as

$$\text{AC}(G_v, G_l) = \mathbb{E}_{c, c' \sim \mathcal{C} \times \mathcal{C}} [\mathbb{E}_{\mathbf{x}_i \sim \mathcal{P}_c} \mathbf{1}[s_{ic} > s_{ic'}]]$$

Therefore our goal is to minimize its gap between the best hind-side subset, for any ρ , without budget constraints,

$$\Delta^\rho(S) = \mathcal{L}_{\text{target}}(\hat{G}_{vl}) - \min_{S' \in D_{\text{train}}} \mathcal{L}_{\text{target}}(\mathcal{A}^\rho(S')), \hat{G}_{vl} = \mathcal{A}^\rho(S)$$

A.2 Generalization Guarantees

We now provide theoretical guarantees and postpone our proof into Appendix A.3. **Firstly, we are going to prove the intuition behind NormSim₂score.**

Lemma A.1 (Intuition behind NormSim₂). *With high probability at least $1 - \frac{1}{|S|^d}$, suppose the hind-side best subset has at least \underline{n} number of samples, then we have*

$$\Delta^\rho(S) = \underbrace{\frac{1}{\rho} \max_{S' \in D_{\text{train}}} (\text{Tr}(\Sigma_{\text{target}}(\Sigma_{S'} - \Sigma_S)))}_{\text{NormSim}_2 \text{ related term}} + \underbrace{\mathcal{O}\left(\sqrt{\frac{d \log(d|S|)}{\underline{n}}} + \sqrt{\frac{d \log(d|S|)}{|S|}}\right)}_{\text{noise}}$$

Proof sketch. ❶ Under the assumption that both $\mathbf{z}^{vl}, \xi_{vl}$ is zero-mean, maximizing the clip score gap is equivalent to maximizing the clip score of the same sample.

$$\mathcal{L}_{\text{target}}(\hat{G}_v, \hat{G}_l) := -\mathbb{E}_{\mathbf{x}^{vl} \sim \mathcal{D}_{\text{target}}} \langle \hat{G}_v^\top \mathbf{x}^v, \hat{G}_l^\top \mathbf{x}^l \rangle$$

❷ By minimizing the regularized training loss $\mathcal{L}_S^\rho(G_v, G_l)$ using Eckart-Young-Mirsky Theorem, we get a closed form solution of \hat{G} as

$$\hat{G}_v \hat{G}_l^\top \approx \frac{1}{\rho} G_v^* \Sigma_S \cdot (G_l^*)^\top + \text{noise depend on } S$$

❸ Combining the result in ❷ and ❶, we have

$$\mathcal{L}_{\text{target}}(\hat{G}_{vl}) \approx -\frac{1}{\rho} \text{Tr}(\Sigma_{\text{target}} \Sigma_S) - \text{noise depend on } S$$

The same analysis can be applied on $\min_{S' \in D_{\text{train}}} \mathcal{L}_{\text{target}}(\mathcal{A}(S'))$ as well. Rearranging these two equations gives us the final result. \square

This lemma shows the $\Delta(S)$ is depend on the NormSim₂-related term and the noise term which comes from ξ . When \underline{n} and $|S|$ is large enough, then the NormSim₂-related term will become dominant. This aligns with our practice experience that the final performance is less sensitive to the small variation in the number of select data as long as that is sufficient. Moreover, in some special cases where test distribution has identity cross-variance, then sampling by greedily choosing CLIP score might be enough.

Now we are ready to give a proof on the choice of $\bar{\Sigma}_{\text{target}}$ and visual-only information. Specifically, the strategy error mainly comes from (1). The unknown test distribution shift from training. (2). The unobservable ground truth Σ_S . To tackle error (1), we assume some prior knowledge on test by using the proxy test variance $\bar{\Sigma}_{\text{target}}$. To tackle the error (2), there are two possible solutions as shown below. Based on the theoretical interpretation, we should choose different strategy based on the property of the teacher embedding model.

$$S_{\text{vision+language}} = \arg \max_S \text{Tr} \left(\bar{\Sigma}_{\text{target}} \left(\sum_{\mathbf{x}^{vl} \in S} \bar{G}_v^\top \mathbf{x}^v (\mathbf{x}^l)^\top \bar{G}_l \right) \right)$$

$$S_{\text{vision only}} = \arg \max_S \text{Tr} \left(\bar{\Sigma}_{\text{target}} \left(\sum_{\mathbf{x}^{vl} \in S} \bar{G}_v^\top \mathbf{x}^v (\mathbf{x}^v)^\top \bar{G}_v \right) \right)$$

Theorem A.1 (Main). *Under the assumption of Lemma A.1,*

$$\Delta^\rho(S) \leq \text{noise} + \frac{1}{\rho} \|\bar{\Sigma}_{\text{target}} - \Sigma_{\text{target}}\| \|\Sigma_S - \Sigma_{\text{best}}\|_*$$

$$+ \frac{1}{\rho} \begin{cases} \epsilon_{v*l}^S & (\text{vision+language}) \\ \epsilon_v^S + \sqrt{1 - \frac{1}{|S|} \sum_{i \in [S]} \langle \mathbf{z}^v, \mathbf{z}^l \rangle} & (\text{vision only}) \end{cases}$$

Firstly, it is evident that the greater the difference between $\bar{\Sigma}_{\text{target}}$ and Σ_{target} , the less improvement we can expect. Moreover, in scenarios where ϵ_l is large (indicating lower accuracy in the language part) while ϵ_v is small (indicating higher accuracy in the vision part), it may be advisable to opt for vision-only embeddings. However, the learner should also consider the term $\sqrt{1 - \frac{1}{|S|} \sum_{i \in S} \langle \mathbf{z}^v, \mathbf{z}^l \rangle}$, which represents the alignment between the ground truth visual and language latent vectors, essentially reflecting the intrinsic quality of the data. If this term is already significant, relying solely on vision information as a proxy for language information could lead to suboptimal results.

A.3 Detailed proofs

Lemma A.2. *Let*

$$\hat{G}_v, \hat{G}_l = \arg \min_{G_v, G_l \in \mathbb{R}^{d \times r}} \mathcal{L}(G_v, G_l) \quad (7)$$

Then we have

$$\hat{G}_v \hat{G}_l^\top = \frac{1}{\rho} G_v^* \Sigma_S (G_l^*)^\top + P_1 + P_2 + P_3 + P_4 \quad (8)$$

where noise terms P_i are defined in (12), (13), (14) and (15).

Proof. Note that $s_{ij} = (\mathbf{x}_j^l)^\top G_l G_v^\top \mathbf{x}_i^v = \text{Tr}(G_v^\top \mathbf{x}_i^v (\mathbf{x}_j^l)^\top G_l)$, like the proof of Corollary B.1. in [42], we have

$$\begin{aligned} \mathcal{L}(G_v, G_l) &= \frac{\sum_{i \in S} \sum_{j \in S} (s_{ij} - s_{ii})}{|S|(|S| - 1)} + \frac{\rho}{2} \frac{|S|}{|S| - 1} \|G_v G_l^\top\|_F^2 \\ &= \frac{\sum_{i \in S} \sum_{j \in S} s_{ij} - |S| \sum_{i \in S} s_{ii}}{|S|(|S| - 1)} + \frac{\rho}{2} \frac{|S|}{|S| - 1} \|G_v G_l^\top\|_F^2 \\ &= -\text{Tr} \left(G_v^\top \left[\frac{1}{|S| - 1} \sum_{i \in S} \mathbf{x}_i^v (\mathbf{x}_i^l)^\top - \frac{|S|}{|S| - 1} \bar{\mathbf{x}}^v (\bar{\mathbf{x}}^l)^\top \right] G_l \right) + \frac{\rho}{2} \frac{|S|}{|S| - 1} \|G_v G_l^\top\|_F^2 \\ &=: -\text{Tr}(G_v^\top \Gamma G_l) + \frac{\rho}{2} \frac{|S|}{|S| - 1} \|G_v G_l^\top\|_F^2 \end{aligned}$$

where $\bar{\mathbf{x}}^{vl} := (\sum_{i \in S} \mathbf{x}_i^{vl})/|S|$. Then by the Eckart-Young-Mirsky Theorem (For example, Theorem 2.4.8 in Golub et al. [43]), we know that

$$\begin{aligned} &\arg \min_{G_v \in \mathbb{R}^{d \times r}, G_l \in \mathbb{R}^{d \times r}} \mathcal{L}(G_v, G_l) \\ &= \arg \max_{G_v \in \mathbb{R}^{d \times r}, G_l \in \mathbb{R}^{d \times r}} \text{Tr}(G_v^\top \Gamma G_l) - \frac{\rho}{2} \frac{|S|}{|S| - 1} \|G_v G_l^\top\|_F^2 \\ &= \{(G_v, G_l) \in \mathbb{R}^{d \times r} \times \mathbb{R}^{d \times r} : G_v G_l^\top = \frac{1}{\rho} \frac{|S| - 1}{|S|} \text{SVD}_r(\Gamma)\} \quad (\text{Eckart-Young-Mirsky Theorem}) \end{aligned}$$

where the notation $\text{SVD}_r(\Gamma)$ means choosing the first r components of the matrix Γ . Further note that

$$\Gamma = \frac{1}{|S|-1} \sum_{i \in S} \mathbf{x}_i^v (\mathbf{x}_i^l)^\top - \frac{|S|}{|S|-1} \bar{\mathbf{x}}^v (\bar{\mathbf{x}}^l)^\top \quad (9)$$

$$=: P_0 + P_1 + P_2 + P_3 + P_4 \quad (10)$$

Here note that $\Sigma_S = \frac{1}{|S|} \sum_{i \in S} \mathbf{z}_i^v (\mathbf{z}_i^l)^\top$, we have P_i as follows:

$$P_0 := \frac{|S|}{|S|-1} G_v^* \cdot \Sigma_S \cdot (G_l^*)^\top \quad (11)$$

$$P_1 := \frac{1}{|S|-1} G_v^* \sum_{i \in S} \mathbf{z}_i^v (\boldsymbol{\xi}_i^l)^\top \quad (12)$$

$$P_2 := \frac{1}{|S|-1} \sum_{i \in S} \boldsymbol{\xi}_i^v (\mathbf{z}_i^l)^\top (G_l^*)^\top \quad (13)$$

$$P_3 := \frac{1}{|S|-1} \sum_{i \in S} \boldsymbol{\xi}_i^{(1)} (\boldsymbol{\xi}_i^{(2)})^\top \quad (14)$$

$$P_4 := -\frac{|S|}{|S|-1} \bar{\mathbf{x}}^v (\bar{\mathbf{x}}^l)^\top \quad (15)$$

It's clear that the rank of the matrix P_0 is no more than r , so $\text{SVD}_r(P_0) = P_0$. And for $i \in \{1, 2, 3, 4\}$, P_i are noise terms with $\mathbb{E}[P_i] = O$. \square

Lemma A.3. For any fixed S , w.h.p $1 - \delta$ the noise term can be upper bounded by $\sqrt{\frac{d \log(1/\delta)}{|S|}}$

Proof. To upper bound the P1 and P2, we have

$$\begin{aligned} \left\| \sum_i \mathbf{z}_i^{vl} (\boldsymbol{\xi}_i^{vl})^\top \right\|_*^2 &= \text{Tr} \left(\sum_{i,j} \boldsymbol{\xi}_i^{vl} (\mathbf{z}_i^{vl})^\top \mathbf{z}_j^{vl} \boldsymbol{\xi}_j^{vl} \right) = \sum_{i,j} (\mathbf{z}_i^{vl})^\top \mathbf{z}_j^{vl} (\boldsymbol{\xi}_j^{vl})^\top \boldsymbol{\xi}_i^{vl} \\ \mathbb{E} \left\| \sum_i \mathbf{z}_i^{vl} (\boldsymbol{\xi}_i^{vl})^\top \right\|_*^2 &= \mathbb{E} \left[\sum_i (\mathbf{z}_i^{vl})^\top \mathbf{z}_i^{vl} (\boldsymbol{\xi}_i^{vl})^\top \boldsymbol{\xi}_i^{vl} \right] = |S|d \end{aligned}$$

Regarding each $(\mathbf{z}_i^{vl})^\top \mathbf{z}_j^{vl} (\boldsymbol{\xi}_j^{vl})^\top \boldsymbol{\xi}_i^{vl}$ as weakly dependent variable, then by using Bernstein inequality, we have, with high probability $1 - \delta$,

$$\left\| \sum_i \mathbf{z}_i^{vl} (\boldsymbol{\xi}_i^{vl})^\top \right\|_*^2 \leq |S|d + \sqrt{d|S|^2 \sigma_\xi^2 \log(1/\delta)} \leq |S|d \sqrt{\log(1/\delta)}$$

So $\frac{1}{|S|} \left\| \sum_i \mathbf{z}_i^{vl} (\boldsymbol{\xi}_i^{vl})^\top \right\|_* \leq \sqrt{\frac{d \log(1/\delta)}{|S|}}$. Note that $\|\bar{\mathbf{x}}^{vl}\| \lesssim \sqrt{\frac{\log(|S|d)}{|S|}}$ (like Proposition 2.5 in Wainwright et al. [44]), it is easy to see that P3 and P4 are the low order terms if $\delta \lesssim \frac{1}{|S|d}$. \square

Lemma A.4 (Intuition behind VAS). With high probability $1 - \delta$, suppose the hind-side best subset has at least \underline{n} number of samples, then we have

$$\Delta(S) = \frac{1}{\rho} \max_{S' \in D_{\text{train}}} (\text{Tr}(\Sigma_{\text{target}}(\Sigma_{S'} - \Sigma_S))) + \sqrt{\frac{d \log(1/\delta)}{\underline{n}}} + \sqrt{\frac{d \log(1/\delta)}{|S|}}$$

Proof. For any learnt G_v, G_l based on dataset S , we have

$$\begin{aligned}
\mathcal{L}_{\text{test}}(G_v, G_l) &= \text{Tr}(G_v^\top \mathbb{E}_{\mathbf{x}_{vl} \sim \mathcal{D}_{\text{target}}} [\mathbf{x}^v(\mathbf{x}^l)^\top] G_l) \\
&= \text{Tr}(\mathbb{E}_{\mathbf{x}_{vl} \sim \mathcal{D}_{\text{target}}} [\mathbf{x}^v(\mathbf{x}^l)^\top] G_l G_v^\top) \\
&= \frac{1}{\rho} \text{Tr}(\mathbb{E}_{\mathbf{x}_{vl} \sim \mathcal{D}_{\text{target}}} [\mathbf{x}^v(\mathbf{x}^l)^\top] G_l^* \Sigma_S (G_v^*)^\top) - \text{Tr}(\mathbb{E}_{\mathbf{x}_{vl} \sim \mathcal{D}_{\text{target}}} [\mathbf{x}^v(\mathbf{x}^l)^\top] \text{noise}_S) \\
&= \frac{1}{\rho} \text{Tr}((G_v^*)^\top \mathbb{E}_{\mathbf{x}_{vl} \sim \mathcal{D}_{\text{target}}} [\mathbf{x}^v(\mathbf{x}^l)^\top] G_l^* \Sigma_S) - \text{Tr}(\mathbb{E}_{\mathbf{x}_{vl} \sim \mathcal{D}_{\text{target}}} [\mathbf{x}^v(\mathbf{x}^l)^\top] \text{noise}_S) \\
&= -\frac{1}{\rho} \text{Tr}(\Sigma_{\text{target}} \Sigma_S) - \text{Tr}(\mathbb{E}_{\mathbf{x}_{vl} \sim \mathcal{D}_{\text{target}}} [\mathbf{x}^v(\mathbf{x}^l)^\top] \text{noise}_S)
\end{aligned}$$

Here the first equation comes from Theorem A.3 and the third equation comes from Lemma A.2. Consequently, we have

$$\begin{aligned}
-\min_{S' \in D_{\text{train}}} \mathcal{L}_{\text{test}}(\mathcal{A}(S')) &= \max_{S' \in D_{\text{train}}} \left(\frac{1}{\rho} \text{Tr}(\Sigma_{\text{target}} \Sigma_{S'}) + \text{Tr}(\mathbb{E}_{\mathbf{x}_{vl} \sim \mathcal{D}_{\text{target}}} [\mathbf{x}^v(\mathbf{x}^l)^\top] \text{noise}_{S'}) \right) \\
&\leq \frac{1}{\rho} \max_{S' \in D_{\text{train}}} (\text{Tr}(\Sigma_{\text{target}} \Sigma_{S'})) + \|\mathbb{E}_{\mathbf{x}_{vl} \sim \mathcal{D}_{\text{target}}} [\mathbf{x}^v(\mathbf{x}^l)^\top]\| \|\text{noise}_{S'}\|_* \\
&\leq \frac{1}{\rho} \max_{S' \in D_{\text{train}}} (\text{Tr}(\Sigma_{\text{target}} \Sigma_{S'})) + \mathcal{O}\left(\sqrt{\frac{d \log(1/\delta)}{n}}\right)
\end{aligned}$$

Therefore, we have the final result as

$$\begin{aligned}
\Delta(S) &= \mathcal{L}_{\text{test}}(\hat{G}_{vl}) - \min_{S' \in D_{\text{train}}} \mathcal{L}_{\text{test}}(\mathcal{A}(S')) \\
&= \frac{1}{\rho} \max_{S' \in D_{\text{train}}} (\text{Tr}(\Sigma_{\text{target}}(\Sigma_{S'} - \Sigma_S))) + \mathcal{O}\left(\sqrt{\frac{d \log(1/\delta)}{n}} + \sqrt{\frac{d \log(1/\delta)}{|S|}}\right)
\end{aligned}$$

□

Theorem A.2 (Main). *Under the assumption of Lemma A.1, we have*

$$\begin{aligned}
\Delta(S) &\leq \text{noise} + \|\bar{\Sigma}_{\text{target}} - \Sigma_{\text{target}}\| \|\Sigma_S - \Sigma_{\text{best}}\|_* \\
&\quad + \begin{cases} \epsilon_{v*l}^S & (\text{vision+language}) \\ \left(\epsilon_v^S + \sqrt{1 - \frac{1}{|S|} \sum_{i \in [S]} \langle \mathbf{z}^v, \mathbf{z}^l \rangle} \right) & (\text{vision only}) \end{cases}
\end{aligned}$$

Proof. Based on Lemma A.1, we will focus on the error cause from selecting subset S , that is, $\text{Tr} \Sigma_{\text{target}} \Sigma_S$. Since the exact Σ_{target} is unknown, we assume the access to some proxy $\bar{\Sigma}_{\text{target}}$ instead.

Recall that, for any S , we have ground-truth $\Sigma_S = \mathbb{E}_{\mathbf{z}_{vl} \in S} \mathbf{z}^v(\mathbf{z}^l)^\top$. Unfortunately, this is not directly observable by the learner. Instead, the learner is able to observe some proxy $\bar{\Sigma}_S$ based on the teacher model \bar{G}_{vl} and therefore solving

$$\arg \max_S \text{Tr}(\bar{\Sigma}_{\text{target}} \bar{\Sigma}_S)$$

and therefore, denote $\Sigma_{\text{best}} = \arg \max_{S' \in D_{\text{train}}} \text{Tr}(\Sigma_{\text{target}} \Sigma_{S'})$

$$\begin{aligned}
\text{Tr}(\Sigma_{\text{target}}(\Sigma_{\text{best}} - \Sigma_S)) &= \text{Tr}(\bar{\Sigma}_{\text{target}}(\Sigma_{\text{best}} - \bar{\Sigma}_S)) + \text{Tr}(\bar{\Sigma}_{\text{target}}(\bar{\Sigma}_S - \Sigma_S)) + \text{Tr}((\Sigma_{\text{target}} - \bar{\Sigma}_{\text{target}})(\Sigma_{\text{best}} - \Sigma_S)) \\
&\leq \text{Tr}(\bar{\Sigma}_{\text{target}}(\bar{\Sigma}_S - \Sigma_S)) + \text{Tr}((\Sigma_{\text{target}} - \bar{\Sigma}_{\text{target}})(\Sigma_{\text{best}} - \Sigma_S)) \\
&\leq \|\Sigma_{\text{target}}\| \|\bar{\Sigma}_S - \Sigma_S\|_* + \|\bar{\Sigma}_{\text{target}} - \Sigma_{\text{target}}\| \|\Sigma_S - \Sigma_{\text{best}}\|_*
\end{aligned}$$

where the first inequality is by the definition of $\bar{\Sigma}_S$ and the second inequality comes from holder's inequality. Now the key is to upper bound $\|\bar{\Sigma}_S - \Sigma_S\|_*$ based on our chosen strategy.

In option 1, we use the clip embedding from both visual and language modal. That is, choose $\bar{\Sigma}_S = \sum_{\mathbf{x}_{vl} \in S} (\bar{G}_v)^\top \mathbf{x}^v(\mathbf{x}^l)^\top \bar{G}_l$. Then we have

$$\|\bar{\Sigma}_S - \Sigma_S\|_* \leq \frac{1}{|S|} \left\| \sum_{\mathbf{x}_{vl} \in S} (\bar{G}_v)^\top \mathbf{x}^v(\mathbf{x}^l)^\top \bar{G}_l - \sum_{\mathbf{x}_{vl} \in S} \mathbf{z}^v(\mathbf{z}^l)^\top \right\|_* \leq \epsilon_{v*l}^S$$

In option 2, we use the clip embedding from language model only. That is choose $\bar{\Sigma}_S = \sum_{\mathbf{x}_{vl} \in S} \bar{G}_v^\top \mathbf{x}^v (\mathbf{x}^v)^\top \bar{G}_v$. Then, by definition of ϵ_S , we have

$$\begin{aligned} \|\bar{\Sigma}_S - \Sigma_S\|_* &\leq \frac{1}{|S|} \left\| \sum_{\mathbf{x}_{vl} \in S} \bar{G}_v^\top \mathbf{x}^v (\mathbf{x}^v)^\top \bar{G}_v - \sum_{\mathbf{x}_{vl} \in S} \mathbf{z}^v (\mathbf{z}^v)^\top \right\|_* + \frac{1}{|S|} \left\| \sum_{\mathbf{x}_{vl} \in S} \mathbf{z}^v (\mathbf{z}^v)^\top - \Sigma_S \right\|_* \\ &\leq \epsilon_v^S + \frac{1}{|S|} \left\| \sum_{\mathbf{x}_{vl} \in S} \mathbf{z}^v (\mathbf{z}^v)^\top - \Sigma_S \right\|_* \end{aligned}$$

Now to further bound the second term, we have

$$\begin{aligned} \frac{1}{|S|} \left\| \sum_{\mathbf{x}_{vl} \in S} \mathbf{z}^v (\mathbf{z}^v)^\top - \Sigma_S \right\|_* &\leq \frac{1}{|S|} \|Z_v^\top\|_* \|Z_v - Z_l\|_* \\ &= \frac{1}{|S|} \sqrt{\text{Tr } Z_v Z_v^\top} \sqrt{\text{Tr } (Z_v - Z_l)^\top (Z_v - Z_l)} \\ &= \frac{1}{|S|} \sqrt{\text{Tr } (I_{n \times n})} \sqrt{2 \text{Tr } (I_{n \times n} - Z_v Z_l^\top)} \\ &= \frac{1}{|S|} \sqrt{2|S|(|S| - \sum_{i \in [S]} \langle \mathbf{z}^v, \mathbf{z}^l \rangle)} \\ &= \sqrt{1 - \frac{1}{|S|} \sum_{i \in [S]} \langle \mathbf{z}^v, \mathbf{z}^l \rangle} \end{aligned}$$

Therefore, we finish the proof. \square

Theorem A.3 (A simplified version of test loss). *Under the assumption that both $\mathbf{z}_{vl}, \xi_{vl}$ is zero-mean, maximizing the clip score gap is equivalent to maximize the clip score of the same sample.*

$$\mathcal{L}_{\text{target}}(G_v, G_l) := -\mathbb{E}_{\mathbf{x}_{vl} \sim \mathcal{D}_{\text{target}}} \langle G_v^\top \mathbf{x}_v, G_l^\top \mathbf{x}_l \rangle$$

Proof. For any \mathbf{x}_{vl} , we have

$$\begin{aligned} &\mathbb{E}_{\mathbf{x}'_{vl} \sim \mathcal{D}_{\text{target}}} (\langle G_v^\top \mathbf{x}_v, G_l^\top \mathbf{x}'_l \rangle - \langle G_v^\top \mathbf{x}_v, G_l^\top \mathbf{x}_l \rangle) \\ &= \langle G_v^\top \mathbf{x}_v, G_l^\top \mathbb{E}_{\mathbf{x}'_{vl} \sim \mathcal{D}_{\text{target}}} (\mathbf{x}'_l - \mathbf{x}_l) \rangle \\ &= -\langle G_v^\top \mathbf{x}_v, G_l^\top \mathbf{x}_l \rangle \end{aligned}$$

\square

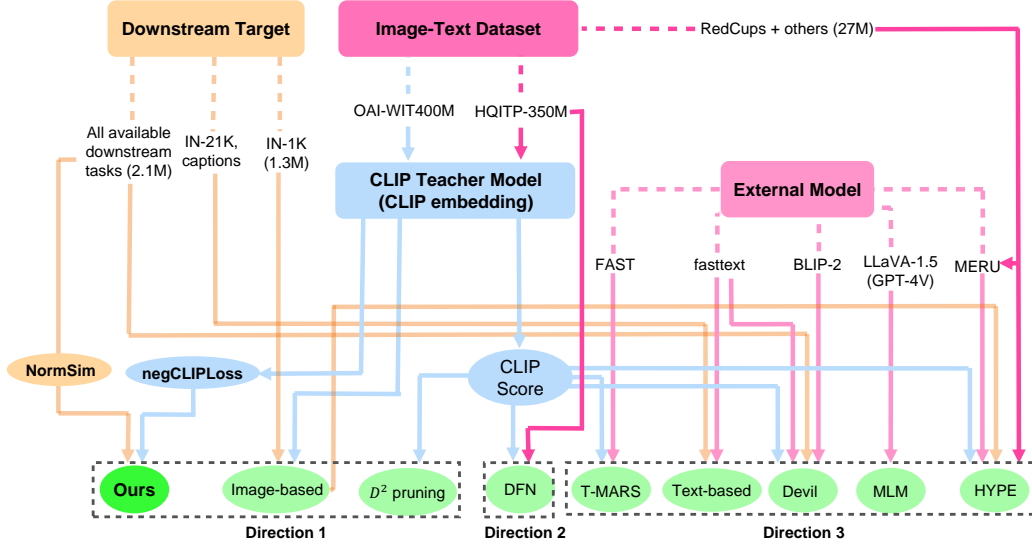


Figure 4: Illustration of different directions for data selection methods for multimodal contrastive learning. Here we use four colors to denote the four main resources we can obtain: CLIP teacher model, downstream target data (which is much smaller than the external multimodal dataset or pretraining dataset), the external image-text dataset, and the external non-CLIP model. **Direction 1** denotes the methods that only use the original OAI CLIP teacher model and the downstream target data. **Direction 2** represents the methods that use external datasets to train a new CLIP teacher model for improving filtering, like DFN [2]. **Direction 3** denotes the methods that use external non-CLIP model to select the data that may be heuristically helpful for downstream tasks, like image without too much text or be more special. In general, *D1 method using only CLIP embedding, like negCLIPLoss, is orthogonal to D2. And both D1 and D2 can be combined with D3 to explore better filtering results.* In the experiments part of the main paper (Sec. 4), we further show that our proposed D1 methods: NormSim and negCLIPLoss, can outperform all the D3 baselines except the best method “HYPE \cup DFN”. And we can achieve the new state-of-the-art by combining our methods with that method.

B Illustration of Different Directions for Data Selection for Multimodal Contrastive Learning

We summarize our main idea of categorizing the current top data selection methods in Table 4.

C Details of Experiments

C.1 Computation Cost

Our algorithm can significantly reduce the computational cost compared to many existing works as shown in Table 4. For example, when the CLIP embeddings are obtained (cost about 50 hours for CLIP-B/32), both T-MARS [8] and MLM [38] still require more than 900 hours data pre-processing time to extract the required information from 110M size dataset of DataComp-medium, while we only need about 5 hours. On the other hand, DFN, although has a similar forward speed (i.e. preprocessing time), requires retraining a new CLIP teacher model on the HQITP-350M, which is larger than DataComp-medium.

We give some details in estimating the preprocessing time of other methods:

- For **T-MARS** and \mathbb{D}^2 pruning, we run their official code on DataComp-small (11M) data, and simply scale the preprocessing time by 10 for DataComp-medium, given that the preprocessing time for T-MARS is proportional to the size of the pretraining dataset, while \mathbb{D}^2 pruning is no faster than linear.

Table 4: Comparison of preprocessing time and external resources needed between our method and other D3 category methods. We skip DFN since it’s orthogonal to our negCLIPLoss method and we can directly improve it as mentioned in Table 2. Here since all the baselines below except MLM use a pretrained CLIP model, we only count the time that doesn’t contain that for inferring CLIP image/text embeddings (about 50 L40 hours for OAI CLIP-B/32), which is also adopted in DataComp benchmark [1]. The external dataset corresponds to the external multimodal dataset used for training or finetuning the external model. Notably, the preprocessing time for the following methods are all approximately linearly proportional to the amount of unfiltered pretrained dataset.

Type	Filtering Strategy	Ext. Model Used	Size of Ext. Dataset	Preprocess Time	Training Time	Avg.
D1	\mathbb{D}^2 Pruning [14]	NA	NA	>70 L40 h	65 L40 h	29.5
D3	T-MARS [8]	FAST [9]	NA	950 L40 h	65 L40 h	34.1
D3	MLM [38]	LLaVA-1.5 [39, 40]	50k	1120 A100 h	65 L40 h	34.5
D3	Devil [10]	fasttext [11], BLIP-2 [12]	NA	510 A100 h	65 L40 h	34.5
D3	HYPE [3]	MERU [41]	27M	> 120 L40 h	65 L40 h	31.9
D1	Ours1	NA	NA	5 L40 h	65 L40 h	35.2

- For **MLM**, we get the estimated time from their paper. They mention that they need 6.1 minutes to process 10k samples on A100, which results in 1120 A100 hours for our dataset (110M). We need to mention that their estimation time of calculating CLIP embedding is inaccurate and we can do it much faster than their claim using the DataComp pipeline.
- For **Devil**, it needs to run the k-means clustering algorithm from the faiss library on the embedding space, which is estimated to cost 120 L40 hours on DataComp-medium. Using BLIP-2 [12] to scan the whole dataset will need about 470 A100 hours from the experimental details in [13]. From <https://lambdalabs.com/gpu-benchmarks>, we roughly assume that 120 L40 hours are at least comparable to 40 A100 hours for K-means clustering.
- For **HYPE**, they claim that MERU is as efficient as CLIP, but they still need at least 120 L40 hours for processing 110M data for their final score, since it uses the image embedding clusters on DataComp-medium obtained from running k-means clustering algorithm.

C.2 Details of negCLIPLoss

In negCLIPLoss, we need to get the batch size $|B|$ and the value of the learnable temperature parameter τ at the final step of the teacher model pretraining stage. For OAI CLIP-L/14 and OAI CLIP-B/32, these values are $\tau = 0.01$ and $|B| = 32768$. We give the pseudocode of calculating negCLIPLoss in Algorithm 1, which is specially designed for pytorch to accelerate matrix calculation. It can be fully accelerated and the computation cost introduced by the normalization term is negligible compared with the training time or preprocessing time of other top baselines as detailed in Table C.1.

C.3 Details of NormSim₂-D

In this section, we illustrate the details of our NormSim₂-D algorithm.

We use greedy remove methods to achieve the object

$$S = \arg \max_{|S|=N} \sum_{i \in S} \bar{f}_v(x_i^v)^\top \left(\frac{1}{|X_{\text{target}}|} \sum_{x_t \in X_{\text{target}}} \bar{f}_v(x_t^v) \bar{f}_v(x_t^v)^\top \right) \bar{f}_v(x_i^v) \quad (16)$$

when the actual X_{target} is unknown. In practice, removing one data at a time is too slow. Therefore, we remove a batch of data for every greedy step. In detail, if the number of greedy steps is τ , and let $\bar{\Sigma}_{\text{test}, i} = \frac{1}{|S_i|} \sum_{j \in S_i} \bar{f}_v(x_j^v) \bar{f}_v(x_j^v)^\top$ where S_i is the selected subset at step i , then we will remove the data satisfies the following equation step-by-step until reaching the final subset size:

$$S_i \setminus S_{i+1} = \arg \min_{x_l \in S_i} \left[\bar{f}_v(x_l^v)^\top \cdot \left(\frac{1}{|S_i|} \sum_{x_t \in S_i} \bar{f}_v(x_t^v) \bar{f}_v(x_t^v)^\top \right) \cdot \bar{f}_v(x_l^v) \right], \quad i \in \{0, \dots, \tau - 1\}$$

Then we can detail the algorithm process of NormSim₂-D in Algorithm 2. In general, the smaller the step size, the better the results. But in experiments, we find that it’s already enough to get good results when greedy steps $\tau = 500$.

Algorithm 1 negCLIPLoss

Inputs: image/text embeddings of the pretraining data $F^{vl} = [\{\bar{f}_{vl}(x_1^{vl})\}, \dots, \{\bar{f}_{vl}(x_N^{vl})\}]^\top \in \mathbb{R}^{N \times d}$, batch size b , temperature parameter τ , the number of times negCLIPLoss is random $K (= 10)$.
Initialize negCLIPLoss array $\mathbf{r} = [0, \dots, 0] \in \mathbb{R}^N$
for $k = 1$ **to** K **do**
 Get a random batch division $S_k = \{B_1, \dots, B_s\}$ such that $s = \lceil N/b \rceil$. Every $B_i \in S_k$ is the index of a batch of data.
 for $j = 1$ **to** s **do**
 Get batch of embeddings in batch j : $F_j^{vl} = F^{vl}[B_j] \in \mathbb{R}^{b \times d}$
 Get the similarity matrix: $E_j = F_j^v (F_j^l)^\top \in \mathbb{R}^{b \times b}$
 Get the CLIP Scores: $\mathbf{c}_j = \text{diag}(E_j) \in \mathbb{R}^b$
 Define $G_j = \exp(E_j/\tau)$
 Define $\mathbf{g}_j^v \in \mathbb{R}^b$ be the vector containing the sum of each row vector in G_j (i.e., over image).
 Define $\mathbf{g}_j^l \in \mathbb{R}^b$ be the vector containing the sum of each column vector in G_j (i.e., over text).

 Get the negCLIPLoss: $\mathbf{r}[B_j] = \mathbf{c}_j - 0.5\tau \cdot (\log(\mathbf{g}_j^v) + \log(\mathbf{g}_j^l))$, here we use element-wise operation.
 end for
end for
Take the mean of each random division as output: $\text{negCLIPLoss} = \mathbf{r}/K$

Algorithm 2 NormSim-D with greedy remove strategy

Inputs: image embeddings of the data after CLIP score filtering $\{\bar{f}_v(x_i^v)\}_{i \in S}$, target size N , number of greedy steps τ
Initialize $S_0 = S, N_0 = |S|$
for $t = 1$ **to** τ **do**
 Size at step t : $N_t = N_0 - \frac{t}{\tau}(N_0 - N)$.
 Prior matrix: $\bar{\Sigma}_{\text{test}, t-1} = \sum_{j \in S_{t-1}} \bar{f}_v(x_j^v) \bar{f}_v(x_j^v)^\top$
 Updated NormSim₂-D for each sample i in S_{t-1} :
$$\text{NormSim}_2\text{-D}(x_i) = \bar{f}_v(x_i^v)^\top \cdot \bar{\Sigma}_{\text{test}, t-1} \cdot \bar{f}_v(x_i^v)$$

 Construct S_t such that it contains the data with highest NormSim₂-D in S_{t-1} and satisfies $|S_t| = N_t$.
end for

C.4 More details in Baselines

We add some details about the baselines used in our paper.

- **Text-based filtering.** [1] proposes a text-based filtering that tries to select the data that contains caption overlapping with the class name from ImageNet-21K or ImageNet-1K.
- **Image-based filtering.** [1] also proposes a heuristic way to sample the visual content overlaps with ImageNet-1K classes. They first apply filtering by language (only choose English caption by fasttext [11]) and caption length (over two words and 5 characters). Then they cluster the image embeddings from training data to 100K groups using Faiss [45], and keep the groups whose cluster center is the nearest neighbor to at least one image embedding of ImageNet-1K image.
- **\mathbb{D}^2 Pruning.** [14] tries to represent the dataset as an undirected graph for coresets selection. They assign the difficulty for each example and use message passing to update the difficulty score incorporating the difficulty of its neighboring examples, and finally try to keep both diverse and difficult subsets. For our experiments, we adhere to the default hyperparameters of \mathbb{D}^2 on DataComp as specified in their official codebase.

- **T-MARS** [8] uses a text detection model like FAST [9] to filter out the data that only contain the texts of caption in the image and don't have other useful image features.
- **Devils** [10] combines many ways for data filtering. At the very first it filter data based on heuristic rules like text length, frequency of texts, and image size, and it also use CLIPScore for cross-modality matchment. Then it adopts target distribution alignment methods similar to image-based filtering, but instead of using ImageNet-1k only, it uses 22 downstream tasks as the target set. Further, it adopts external models fasttext [11] to remove non-English captions and image-captioning model BLIP-2 [46] to select images with MNIST-style digits.
- **MLM** [38] prompts GPT-4V to construct instruction data including the image-text data, and use it to fine-tune a smaller vision-language model like LLaVA-1.5 [39, 40] into a filtering network. Nevertheless, the number of parameters of LLaVA-1.5 is still much larger than CLIP, and thus LLaVA-1.5 has a much longer preprocessing time as mentioned in Table C.1.

C.5 Hyperparameters

The main hyper-parameters of our negCLIPLoss and NormSim are the target numbers for filtering, which is also the main concerns for all the top baselines like DFN, MLM, and T-MARS. However, from the current paper about the scaling law for data filtering [47], the downsampling size should depend on the computation budget. When you have more budget, you should sample more data for learning. And we can use their fitting formula to get some good downsampling ratios.

In the case of the DataComp benchmark, however, we can set the sampling ratio as some previous baselines. but in general, for NormSim, we can also filter out the data until some **train-dataset-independent** threshold since this score only depends on the norm p and target data. For example, we find it good to set the threshold as **0.7** for **NormSim_∞(Target)** and **0.15** for **NormSim₂(IN-1k)**. For negCLIPLoss, we can find a similar way: first find the ratio of data whose CLIP score is higher than **0.21**, then use this ratio to filter negCLIPLoss.

Besides, we found an effective parameter tuning way particularly for data selection problems, that is, visualization. First randomly selecting a small subset (like 1000 data) on some pretraining data subset and calculating the target metric on them, then visualizing the data with different scores, it turns out to be a very effective way to give some guidance on how to select the downsampling ratios.

D Additional Results

D.1 Stability Analysis of Batch Sampling Numbers in negCLIPLoss

We show that negCLIPLoss is not sensitive to the number of random select batches K in Figure 5.

D.2 Universality of negCLIPLoss over Different Teacher Models

We show the complete results of applying our methods to different teacher models like OAI CLIP-B/32 and DFN-P in Table 5. Detail descriptions are in Sec. 4.

D.3 NormSim_∞ is Better than Nearest Neighbor Selection

We also try to use near-neighbor selection for aligning downstream distribution. Here, we calculate the ranks of pretraining data for each target (the higher the rank, the higher the similarity), and then for each pre-train data, we keep its highest rank. Finally, we select the data with the highest ranks as the nearest neighbor selected subset.

In Table 6, we show that given the training data of 22 downstream tasks, our NormSim_∞ can outperform near neighbor selection under the same downsampling ratio. The reason may be that the distribution between the target and pretraining set is not well aligned, so if you force the algorithm to find the nearest train data for each target, that train data may be sometimes random and not helpful. On the other hand, NormSim_∞ will not select this kind of data. It will select the data whose best similarity score exceeds some general threshold, rather than just consider ranks.

Comparison of Methods Across Different Metrics

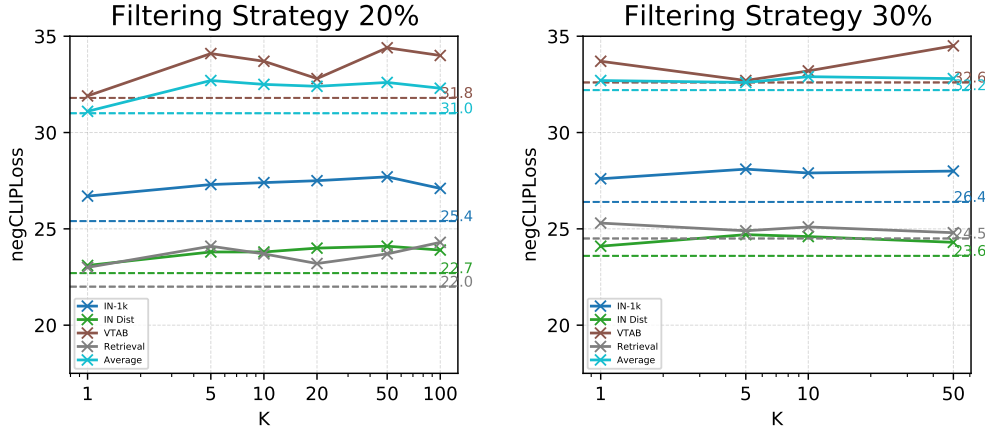


Figure 5: Results of negCLIPLoss with a different number of batch samples (denoted as K) on DataComp-medium. Solid lines denote negCLIPLoss, while dashed lines denote CLIPScore. Here, we use OAI CLIP-L/14 as the pretrained model. We can see that once $K \geq 5$, negCLIPLoss consistently outperforms CLIPScore across all subtask metrics. In the main paper, we set $K = 10$.

Table 5: Results on DataComp-medium from the top methods that use only OpenAI’s CLIP-B/32 model or public version of DFN (DFN-P).

OAI CLIP-B/32	Dataset Size	IN-1k (1 sub-task)	IN Dist. Shift (5)	VTAB (11)	Retrieval (3)	Avg. (38)
CLIPScore (20%)	22M	27.0	23.8	33.0	22.9	32.2
CLIPScore (30%)	33M	27.6	24.2	33.6	25.1	33.2
negCLIPLoss (20%)	22M	28.9	24.8	34.3	24.3	33.0
negCLIPLoss (30%)	33M	28.8	25.1	33.7	26.6	33.6
negCLIPLoss (30%) \cap NormSim $_{\infty}$ (Target)	22M	32.4	27.4	35.9	26.3	35.2
DFN-P						
CLIPScore (15%)	16M	25.9	23.3	32.9	21.9	31.6
CLIPScore (17.5%)	19M	30.2	26.8	34.1	26.5	33.8
CLIPScore (20%)	22M	29.7	26.8	33.0	27.0	33.1
CLIPScore (30%)	33M	28.4	24.7	33.2	26.8	32.7
negCLIPLoss (15%)	16M	31.3	27.3	35.8	26.4	34.6
negCLIPLoss (17.5%)	19M	31.2	27.5	35.7	27.0	34.7
negCLIPLoss (20%)	22M	30.7	<u>27.4</u>	33.6	27.5	33.8
negCLIPLoss (30%)	33M	28.9	25.5	33.4	27.3	33.2
negCLIPLoss (30%) \cap NormSim $_{\infty}$ (Target)	22M	29.4	23.6	33.5	24.2	32.5
negCLIPLoss (17.5%) \cap NormSim $_{\infty}^{B/32}$ (Target)	16M	31.6	27.3	37.2	25.5	35.7

D.4 Vision-Only NormSim is Better than Using Both Vision and Language

In DataComp [1], they show that image-based filtering is better than text-based filtering. In our paper, we also do an ablation study to support this. Due to the restriction of computation resources, we run our NormSim₂(IN-1k) and NormSim₂-D on DataComp-small as an example. Since ImageNet-1k only has labels rather than long texts for describing images, we need to generate the caption before calculating NormSim₂(IN-1k). We select 80 templates as the original CLIP paper [4], generate prompts for each class, and take the mean of their embeddings as the representative text embedding for images within that class.

Table 6: Comparison between NormSim_∞ and nearest neighbor selection. We use OAI CLIP-L/14 as the teacher model and assume both methods have been intersected with negCLIPLoss (30%). The size of the selected subset is 22M.

Filtering Strategy	IN-1k	VTAB	Avg.
negCLIPLoss (30%)	27.9	33.2	32.9
Nearest Neighbor Selection	31.5	34.9	34.0
NormSim _∞ (Target)	31.7	36.0	35.0

The results are in Table 7. We can see that for both metrics, we have “**image only**” > “**image × text**” > “**text only**”. We believe the reason for NormSim₂(IN-1k) is that the images themselves can convey significantly more features than the text prompts generated by labels. For NormSim₂-D, it should be related to the large amounts of low-quality captions in the web-curated dataset. And “image × text” will also be influenced by the informativeness and the quality of captions. In short, for NormSim, using vision-only embeddings is a best choice.

Table 7: Ablation Study on the NormSim and its variants on DataComp-small (11M). All experiments first select 45% data based on the CLIP score, then use corresponding approaches to obtain 3.3M data. “image” or “text” means using the variance of image or text embeddings to represent $\bar{\Sigma}_{\text{target}}$, and “image × text” means representing $\bar{\Sigma}_{\text{target}}$ with the cross-covariance of image and text embeddings.

Filtering Strategy \cap CLIP score (45%)	IN-1k	IN Dist. Shift	VTAB	Retrieval	Average
Random Sampling	4.2	4.9	17.2	11.6	15.6
NormSim (IN-1k, image)	5.2	5.5	<u>19.0</u>	12.2	17.4
NormSim (IN-1k, text)	3.9	4.2	<u>16.3</u>	11.3	14.9
NormSim (IN-1k, image × text)	4.3	4.9	17.5	<u>11.8</u>	15.9
NormSim-D (image)	<u>4.7</u>	<u>5.4</u>	19.7	11.7	<u>17.3</u>
NormSim-D (text)	3.5	4.1	16.7	11.1	15.4
NormSim-D (image × text)	3.6	4.2	18.4	11.1	15.8

E Additional Visualization

We further visualize more data with different negCLIPLoss in Figure 6, 7 and 8. And similar for NormSim_∞(Target) in Figure 9, 10 and 11.

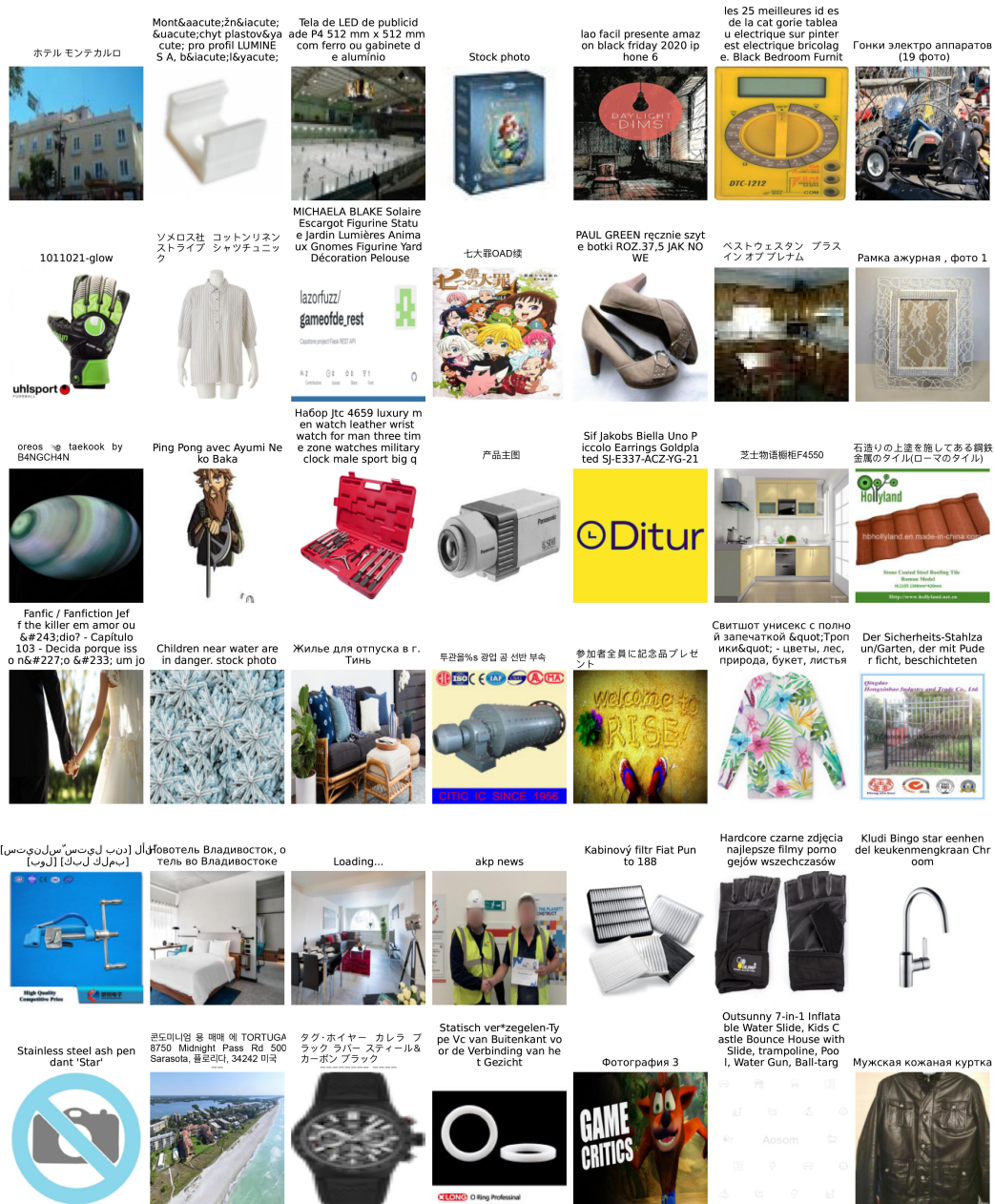


Figure 6: Visualization of a small subset whose negCLIP loss rank top 100% high in DataComp-medium.

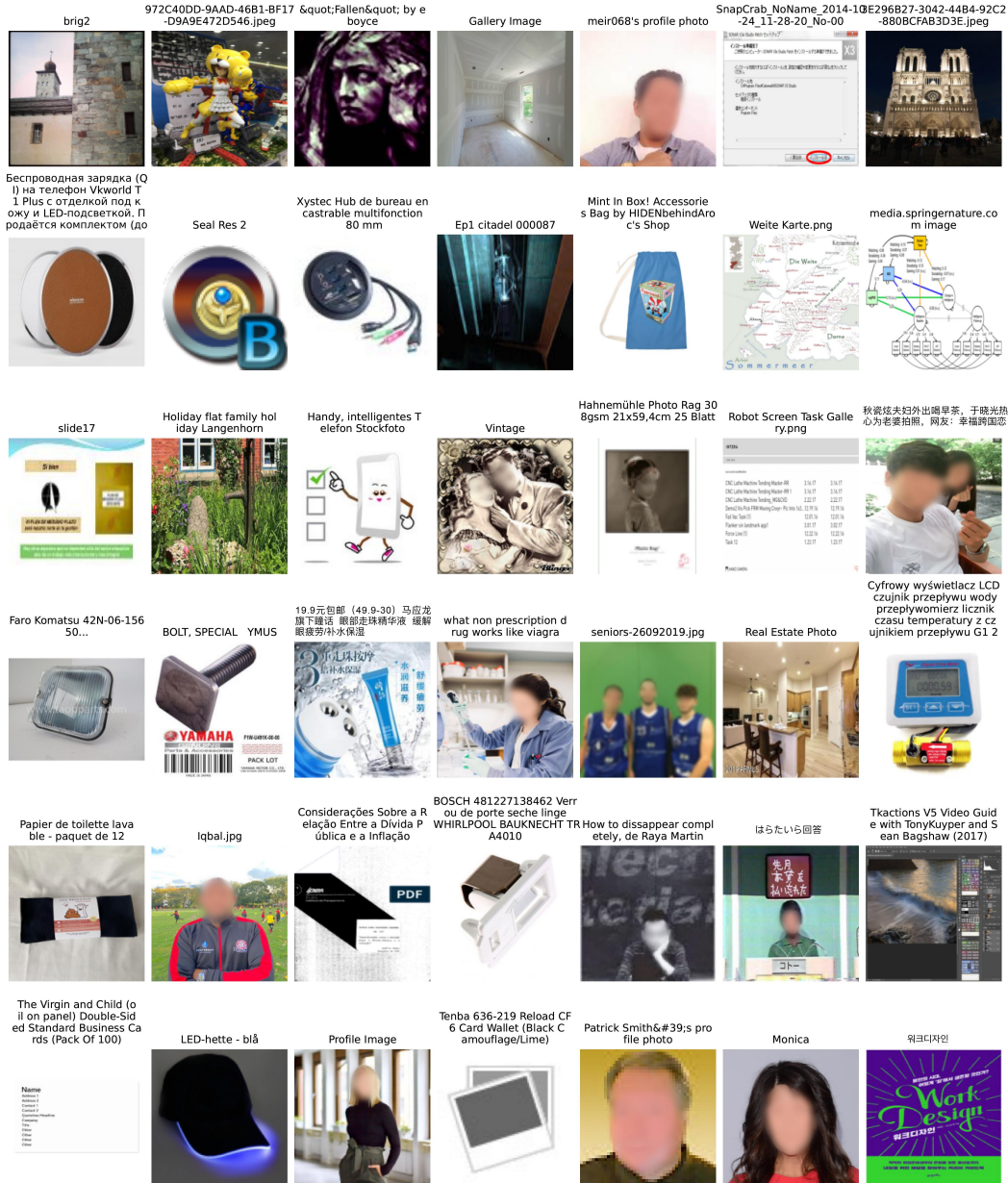


Figure 7: Visualization of a small subset whose negCLIPLoss rank top 50% high in DataComp-medium.

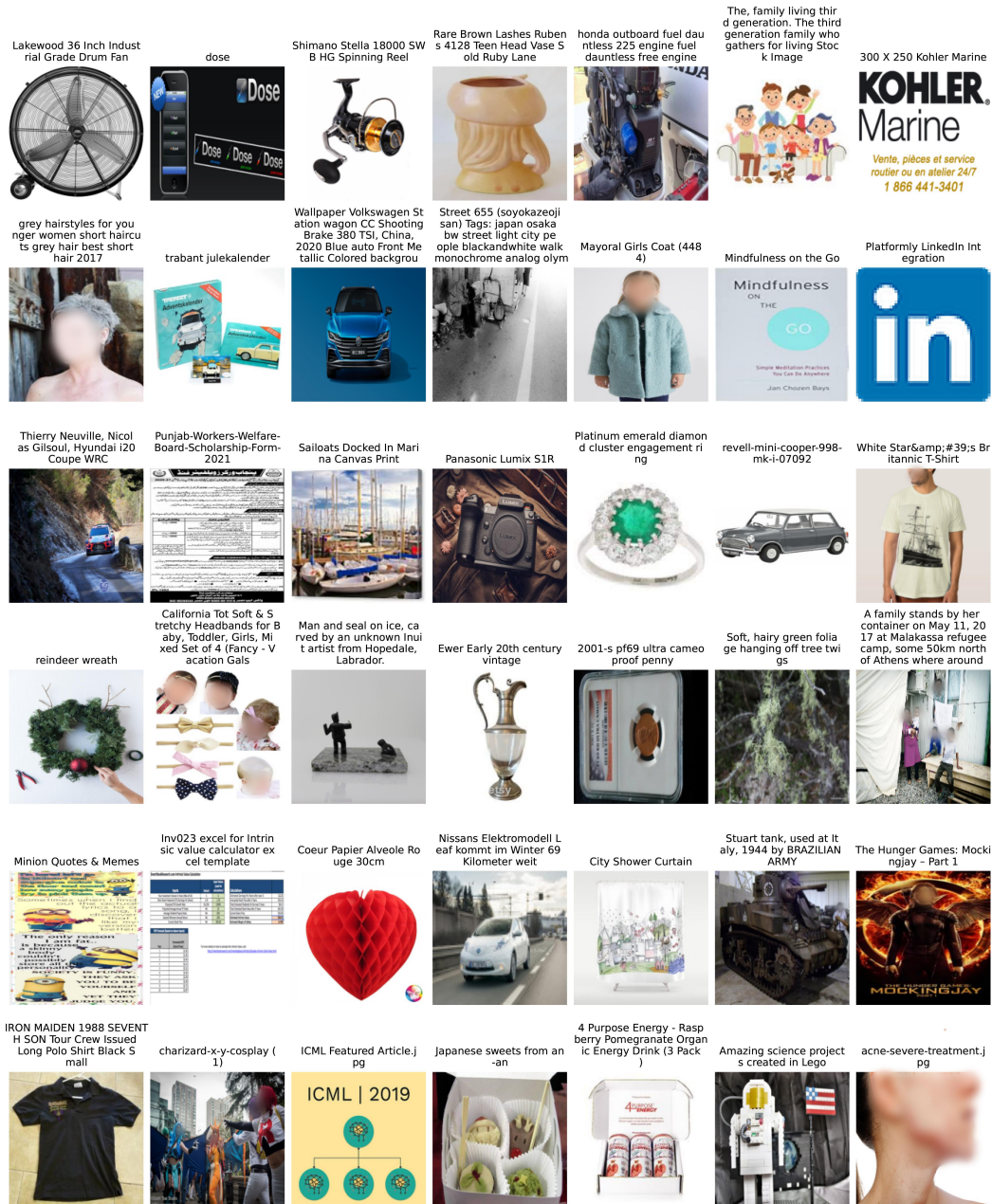


Figure 8: Visualization of a small subset whose negCLIP loss rank top 10% high in DataComp-medium.



Figure 9: Visualization of the images from a small subset whose $\text{NormSim}_\infty(\text{Target})$ rank top 100% high in DataComp-medium.

